MASTER PROGRAM IN

INTERNATIONAL STUDY IN

PETROLEUM ENGINEERING

Development of an Energy Consumption Model

Based on Standard Drilling Parameters

Dipl. Ing. Gabriel Gomes Müller

Leoben, June 2015

UNIVERSITY OF LEOBEN

MASTER PROGRAM IN
INTERNATIONAL STUDY IN
PETROLEUM ENGINEERING

Development of an Energy Consumption Model

Based on Standard Drilling Parameters

Master Thesis submitted to the Master Program in International Study in Petroleum Engineering as partial fulfillment of the requirements for the title award Master of Science (M.Sc.) in International Study in Petroleum Engineering.

Degree emphasis module: Drilling Engineering

Supervisor: Univ.-Prof. Dipl.-Ing. Dr.mont. Gerhard Thonhauser

Co-supervisor: Prof. Dr. Edson da Costa Bortoni

June 2015

“There are men who struggle for a day, and they are good. There are others who struggle for a year, and they are better. There are some who struggle many years, and they are better still. But there are those who struggle all their lives, and these are the indispensable ones.”

Bertolt Brecht

DEDICATORY

This thesis is dedicated to my parents who have supported me all the way since the beginning of my studies.

Also, this thesis is dedicated to Elena who has been a great source of motivation and inspiration.

Finally, this thesis is dedicated to all those who believe in the richness of learning.

Affidavit

I declare in lieu of oath, that I wrote this thesis myself and have not used any sources other than quoted at the end of the thesis. This Master Thesis has not been submitted elsewhere for examination purpose.

Ich erkläre hiermit Eides statt, die vorliegende Arbeit eigenhändig, lediglich unter Verwendung der zitierten Literatur angefertigt zu haben. Diese Diplomarbeit wurde nirgends sonst zur Beurteilung eingereicht.

Leoben, June 28, 2015

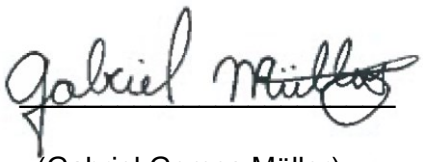

(Gabriel Gomes Müller)

ACKNOWLEDGEMENTS

To Univ.-Prof. Dipl.-Ing.Dr.mont. Gerhard Thonhauser (MUL) and Prof. Dr. Edson da Costa Bortoni (UNIFEI), for the orientation, guidance, patience, and support while developing this research.

To Univ.-Prof. Dipl.-Ing.Dr.mont. Herbert Hofstätter, Ass.Prof. Dipl.-Ing. Dr.mont.Michael Prohaska-Marchried, Dipl.-Ing.Dr.mont. Stefan Wirth from MUL and to Dr. Antonio Claret Silva Gomes, for all the attention provided over this degree.

To all employees and professors from the University of Leoben (Montanuniversität Leoben, MUL). To all employees and professors from the Federal University of Itajubá (Universidade Federal de Itajubá, UNIFEI).

To all friends, especially those from Leoben, for following up and believing in the development of this work. Thank you very much Elena Chevelcha for your exceptional support.

To all my colleagues at TDE, who supported me.

To my family, for their help and encouragement in developing this thesis.

Abstract

Current lower oil price has thrown energy efficiency into sharp focus. The author believes that the drilling industry should have a responsibility to minimize cost and maximize efficiency in all circumstances. The thesis develops methods to quantify energy consumed for drilling as a potential drilling optimization. For this purpose, energy consumption models are developed and empirical measurements are made to track performance against the model.

General energy consumption concepts are used to develop three mathematical energy consumption models for each of the major energy consumers of a rig: mud pumps, top drive and draw-works. Thesis includes justification and explanation of developed models with supporting theory. The research also includes a chapter dedicated to models confirmation, verification and validation, where modeled fuel consumed results are cross referenced against the real fuel consumed data. These steps gradually prove accuracy of the created energy consumption models.

As a result, the thesis proves the possibility to use the drilling parameters to accurately calculate the energy consumption for each phase of rig activity. Thesis also offers to improve models by enhancing drilling data quality and drilling rig specifications. Additionally, the author suggests the further application of the research in the area related to drilling energy efficiency KPIs.

LIST OF FIGURES

LIST OF TABLES

LIST OF EQUATIONS

CONTENT

1. Introduction

The climate of drastically dropping oil price reminds to the oil companies that any penny saved is a penny earned. Due to historical oil price fluctuations the topic of drilling efficiency became important in terms of determining the commerciality of drilling in field development activities. The energy consumption is a great contributing factor of the operational drilling cost as it accounts for 10-30% of the operational cost, thus, energy efficiency of a drilling rig is a vital point (Cherutich, 2009). Especially, this becomes essential when discussing large scale field development of unconventional resources, which frequently have high drilling intensity and an elevated cost per barrel ratio. Thus, the knowledge regarding the energy required to drill a well, and monitoring of its consumption can improve understanding of the well profitability and drilling process. Energy efficiency in the drilling phase has the potential to reduce overall development Capital Expenditure. By using information about energy required to drill a well, drilling engineers can take leading decisions in terms of type of equipment to use (e.g. type of drill bits, top drives), rate of penetration (faster may not mean better), drilling mud pumping rate, among others. Beyond commercial benefits, improved energy efficiency can also reduce the carbon footprint for development drilling activity. The considerable message of the thesis is to underline the importance of managing energy consumption in drilling activities.

The idea of the thesis is to support a PhD student of the University of Leoben (Montanuniversität Leoben), MSc Mathias Mitschanek, in the research related to the simulation of the development of large unconventional fields. Thus, the thesis focuses on a part of this macro model in regards to energy consumed during the well construction phase.

Drilling process can be described with the help of eight drilling parameters, which are measured at the rig site with the help of sensors (this is shortly mentioned in the thesis) and are used to calculate Key Performance Indicators (KPIs). KPIs are monitored, recorded and stored during each phase of the drilling process and can be used to improve performance. Since the drilling parameters are common and trusted data gathered on the rig site, they are taken to be used as an input parameter for the energy consumption model of a drilling rig in this thesis.

During the drilling process, there are four major energy consumers detected: mud pumps, top drive, draw-works, and extra equipment. Knowledge of their specification, performance and interconnection together with the available drilling parameters is applied to solve the energy consumption task. Having indicated that, the thesis concentrates on the following specific objectives:

- To develop a mathematical model that represents each of the major energy consumers in a rig (pumps, top drive, draw-works);
- To develop a integration of the models and provide a final result of energy consumed;
- To construct a process that validates the developed models.

1.1 Thesis structure

The thesis is structured as follows:

In this first chapter, Introduction, aspects of the thesis as its structure, purpose and a brief background of the subject and its importance are addressed.

Chapter two presents an overview of drilling rig system and its components; drilling sensors and drilling data acquisition; detailed description of the equipment that are the main energy consumers of a drilling rig: top drive, mud pumps and draw-works.

Chapter three describes the Energy Consumption Model that was developed in this thesis with the objective to simulate the energy consumption of a drilling rig. The chapter is divided into three sections. The first section defines all input data, which are necessary to run the model. The second section explains necessary concepts (e.g. energy, power, efficiencies, among others) and equations used to develop the model. The third section deals with each component used for mathematical model and describes them particularly. This section is sub-divided into five sub-sections. The first four present a detailed description of the steps taken to calculate the total electrical power requirements for each of the four sub-models (i.e. top drive, mud pumps, draw-works and extra equipment). The last sub-section presents an integration of the four sub-models into one final result of total energy required per unit of time.

Chapter four is created to perform the Accreditation of the Energy Consumption Model through the process of Confirmation, Verification and Validation (CV&V). Firstly, the model CV&V process concepts are explained, after a description of the implementation of this process in the model developed and the results obtained.

Chapter five includes conclusions and further work recommendations of the thesis.

2. Drilling Rig System

This chapter presents an overview of the drilling rig system, the sensors which are used to record drilling data, and a more detailed description of the equipment which represent the major energy consumers as part of a typical rig system.

2.1 Drilling Rig

A drilling rig is a machine which creates holes in the ground in order to extract oil, gas or any other natural resources from the subsurface. Drilling rigs are structures that house equipment used to drill water wells, oil wells, or natural gas extraction wells. Drilling rigs can be mobile equipment mounted on trucks, tracks or trailers, or more permanent land or marine-based structures (such as oil platforms, commonly called 'offshore oil rigs' even if they do not contain a drilling rig). The term "rig" therefore generally refers to the aggregate of equipment that is used to penetrate the surface of the Earth's crust.

Numerous sensors are mounted at the rig to record different physical parameters during drilling, such as block position, hookload, mud pumps flow rates, mud pumps pressure, hole depth, bit depth and torque, among others.

Over the years, with the continuous development of new technology, different types of drilling rigs were developed. Drilling rigs tend to be classified by the type of power used to operate the equipment on the rig (Besore, 2010):

- Mechanical rigs use dedicated diesel engines to provide motive force for the mud pumps, draw-works, rotary drill table, and other loads through a system of clutches and transmissions.
- Hydraulic rigs have dedicated diesel engines running hydraulic pumps, which provide power to the necessary equipment.
- DC/DC or AC/DC electric rigs use dedicated diesel-electric direct-current generators to power DC motors that run the equipment.
- AC electric rigs use dedicated diesel-electric alternated-current generators to power AC motors that run the equipment.

Today, the latest technology available on the market is the AC drilling rig with variable frequency drive (VFD). For this type of a rig all the equipment uses the AC current.

This thesis focuses on the “State of the Art” of the technology that is the AC drilling rig. Figure 1 represents a general schematic of an AC drilling rig and its main components.

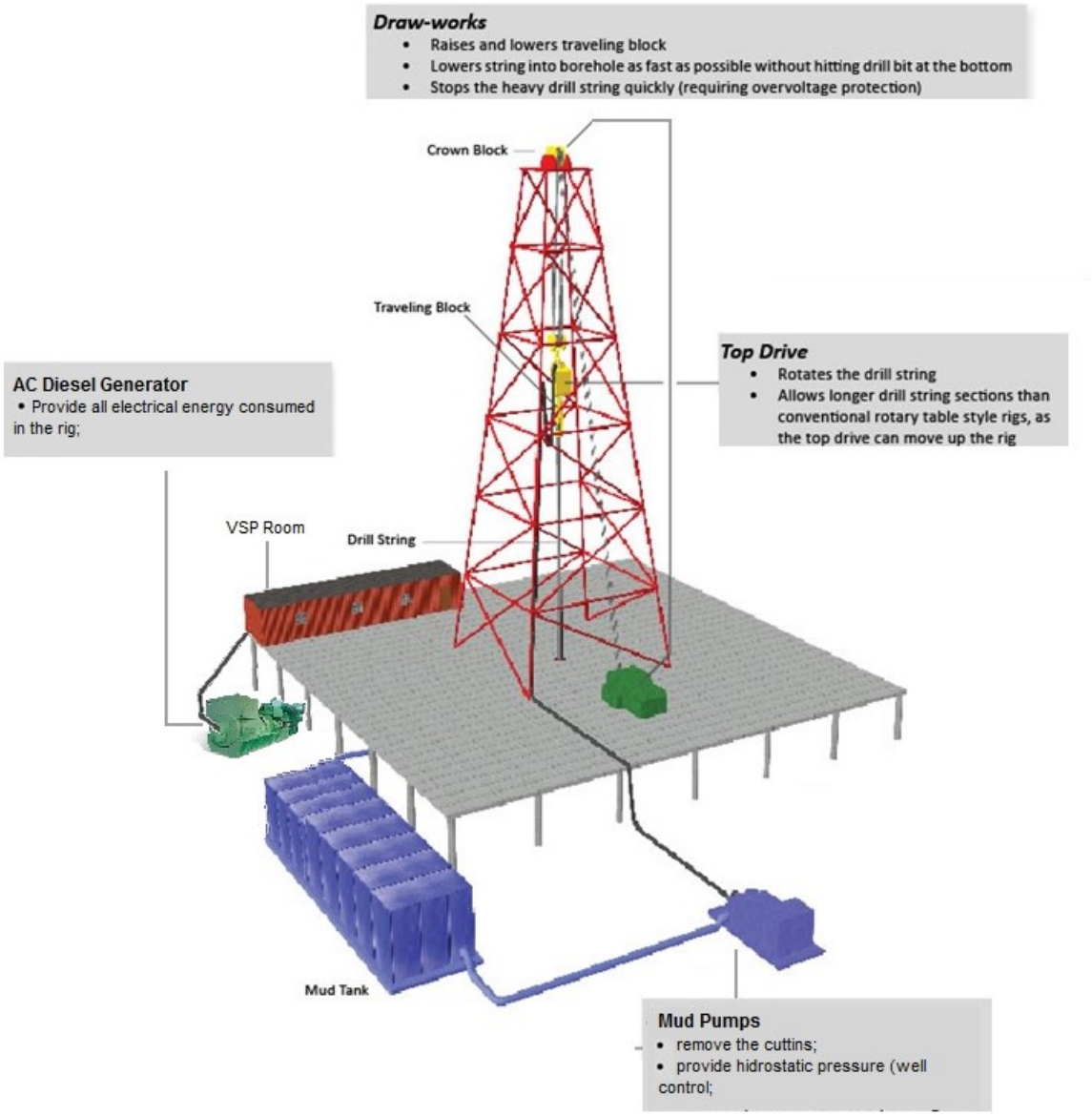

Figure 1: AC drilling rig with main components (Source: modified from Bonitron Inc., 2014).

2.1.1 AC Drilling Rig

The unconventional resource boom that has revolutionized the oil and gas industry also is responsible for the on-shore drilling rig fleet transformation.

An overwhelming shift in well orientation towards horizontal drilling and consequent enhancements in drilling efficiencies have been key to rendering unconventional oil and gas resources economic. Incremental improvements to horizontal drilling and hydraulic fracturing technologies have, in essence, enabled operators and drillers to economically develop source rock. Such a concept – unthinkable not that long ago – has turned the U.S. energy outlook up-side down, and completely changed U.S. crude oil, natural gas and natural gas liquids supply.

However, one fundamental change is already apparent: the type of drilling rig that long dominated the land rig fleet is relinquishing its role. Bigger-horsepower, higher-tech rig designs are the new order of the day. These are the types of rigs favored by the horizontal unconventional drilling business model, which will increasingly come to define hydrocarbon exploration and development in general. The fleet transformation also includes automated, highly portable rigs that enable a two- or three-man crew to do what once required fiveto six-man crew on the floor.

These trends are manifesting themselves in a major rig replacement cycle. Many land rig contractors are in the process of upgrading their U.S. land drilling fleet with higher-horsepower new-builds, adding more powerful rigs with advanced technological capabilities– from top drives to automated pipe handling, and the mobility to quickly move from well site to well site.

Advances in technology related to key rig components are underpinning the shift toward long-lateral horizontal drilling in unconventional gas and now oil reservoirs are creating a new model for drilling rig design: AC power systems.

The inherently simpler design of an AC rig, with its lighter weight and reduced maintenance requirements, also makes it better suited to automation. Nabors states that AC electrical systems provide more accurate control of speed and torque than DC (Oil & Gas Journal, 2006). AC electrical systems also require less maintenance and facilitate online diagnostic checks of equipment and systems. AC-powered drilling rigs have fewer electrical connections and better motor efficiency and produce less noise and fewer emissions, enjoy better power distribution, says the company.

The programmable AC electric rigs incorporate programmable logic controllers (PLC), which the company says allow the driller to control the draw-works, top drive, pipe-handling equipment, mud pumps, and many other systems from a central control center and remote locations. PLC facilitates integrated systems for anti-collision, over pull limits, and automated alarms. The heart of the PLC system is the variable frequency drive (VFD) room, containing circuitry for the entire rig.

Drilling rigs have several electrical components, and only three of them are responsible for the consumption of 85-95% of electric power. Figure 1shows schematic of an AC Electric Rig Design, where the three main energy consumer of a rig are indicated.

2.2 Rotary System

The function of the rotary system is to transmit rotation to the drill string and consequently rotate the bit, which in turn digs the hole deeper and deeper into the ground. The rotating equipment consists of a number of different parts, all of which contribute to transferring power from the prime mover to the drill bit itself (e.g. swivel, rotary hose, top drive).

The prime mover supplies power to the top drive, this can be powered by hydraulic or electric motors. The top drive is suspended in the rig mast, above the drill pipe and enables to rotate and pump through the drill string continuously while drilling or during the removal of a drill pipe from the hole. A component called swivel, which is attached to the hoisting equipment, carries the entire weight of the drill string, but allows it to rotate freely.

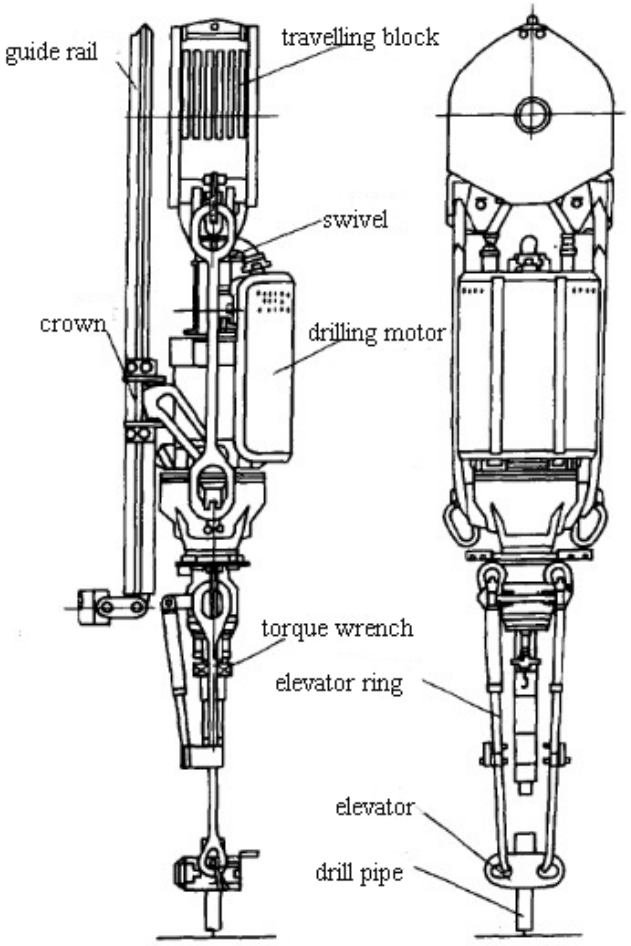

Figure 2: Rotary system (Source: China-OGPE, 2013).

2.2.1 Top Drive

A top drive provides clockwise torque to the drill string and consequently the drill bit to facilitate the process of drilling a borehole. The top drive system replaces the functions of a rotary table, allowing the drill string to rotate from the top.

A top drive is comprised of one or more electric or hydraulic motors, which is connected to the drill string via a short section of pipe known as the quill. Suspended from a hook below the traveling block, the top drive is able to move up and down the derrick.

One of the biggest benefits of using a top drive is this ability to drill with stands, typically eliminating two-thirds of all connections. This saves time and reduces the chance of downhole problems. Other benefits of drilling with a top drive include:

- The possibility to back-ream, allowing full rotation and circulation while tripping out
- Reduce the risk of entrapment of the string, for their ability to rotate and move at the same time.
- Improved well control since stabbing is instant and the well can be shut in at any position in the derrick.
- Increased safety due to one back-up tong being required and fewer pipe connections.
- Easily installed on any mast or derrick, with minimal changes and often within a single day.
- “Improving safety in the handling of the pipe”. All operations are performed remotely from the driller’s cabin, reducing manual tasks and risks that traditionally accompany the task.
- Perform core taken at intervals of 90 feet without having to make connections.
- In directional drilling, maintaining the orientation at intervals of 90 feet, reducing the monitoring time (survey time) improved directional control.
- Ability to tighten the connection by giving them a proper torque.

Several different kinds of top drives exist and are usually classified based on the "Safe Working Load" (SWL) of the tool, and the size and type of motor used to rotate the drill pipe. For offshore and heavy duty use, a 1000 HP, top drive would be used, where a smaller land rig may only require a 500 HP. Motors are available in all sizes and come in hydraulically powered, AC, or DC motors.

2.2.2 RPM Sensor

A RPM sensor is located at the top drive which measures the number of revolutions of a drill-string per time, usually per minute (rpm). The sensor used can be a proximity sensor that is connected to the top drive for counting the revolutions of the drill string.

2.2.3 Torque Sensor

The torque sensor represents the moment of a force applied to the drill string to produce torsion and rotation. Usually this is often obtained from an electrical measurement in the powered portion of the top drive. Usual way to measure torque on rigs is to use the toroidal magnetic field (a.k. a “donut”), surrounding one of the power leads of the motor. Current passing through the magnetic field induces a voltage in the sensor. These readings are then compared to the motor manufacturer’s operational data (Florence & Iversen, 2010).

2.3 Hoisting System

The hoisting system works as an elaborate pulley to lower and raise the drill string, casings, and other subsurface equipment into or out of the well. Figure 3 shows the hoisting system at the drilling rig. The hoisting system consists of the derrick, traveling and crown block, the drilling line, the draw-works, among others. The drilling rig uses a derrick to support the drill bit and the pipe (drill string). The derrick is a steel tower that is used to support the traveling and crown block and the drill string. There may be no more identifiable symbol of the oil and gas industry then the derrick of a drilling rig.

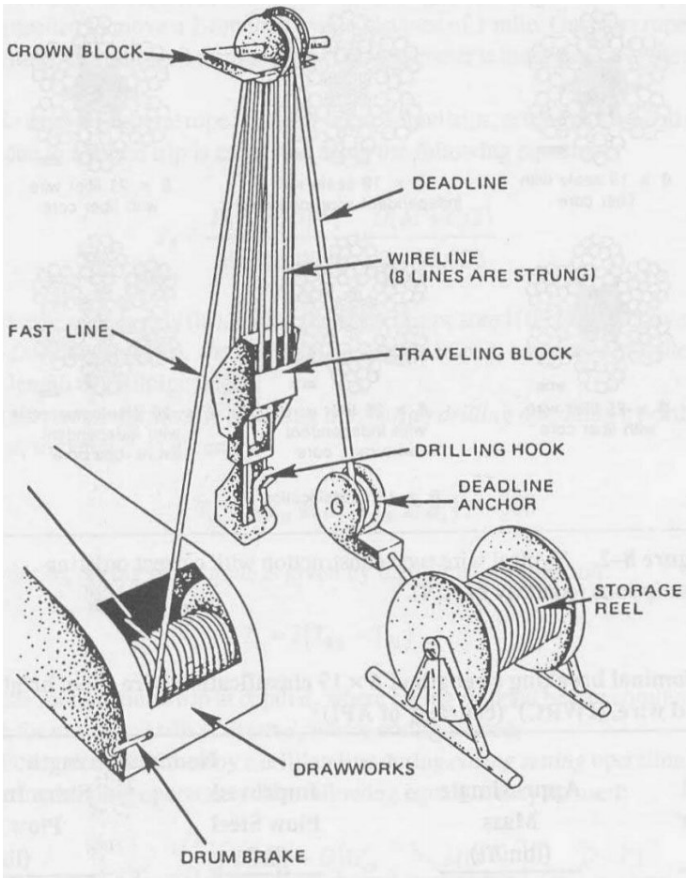

Figure 3: Hoisting system schematic (Source: Prassl, 2002).

The traveling and crown blocks are a group of pulleys that are used to raise and lower the drill string in the well. The travelling block moves up and down in the derrick and it is used to raise and lower the drill string. The crown block is a stationary, located at the top of the derrick. The blocks are connected to each other via a large diameter steel cable, which is connected to the draw-works.

2.3.1 Draw-works

The main function of the draw works is to reel the drill line in or out, to raise or lower the travelling block which is coupled to the drill string thus enabling it to run in hole, and to pull

out of the hole, or drilling by giving the weight on the bit to exert the force. The draw-works consists of: (1) Driller's console, (2) Spinning cathead, (3) Sand reel, (4) Main drum (grooved), (5) Hydromatic Brake and (6) Manual breaks (see Figure 4).

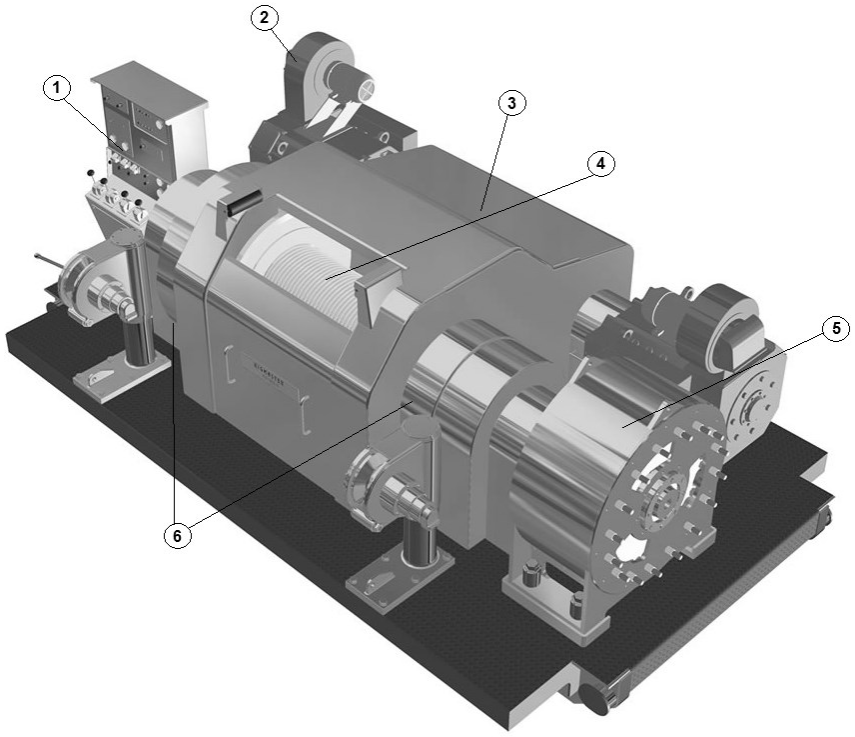

Figure 4: Draw-works (Source: modified from Rigmaster Machinery Ltd., 2013).

The drum provides the movement of the drilling line which in turn lifts and lowers the travelling block and consequently lifts or lowers the loads on the hook. The breaking torque, acting at the drum, has to be strong enough to be able to stop and hold the heavy loads of the drilling line when lowered at high speed (Cherutich, 2009). The power required by the draw-works can be calculated when considering the hookload and travelling block speed.

The draw-works is equipped with independent numerical-control AC-VF transmission device and automatic control system (ACS). The main brake of the draw-works is hydraulic disc brake while the auxiliary brake is an energy consumption brake, or EATON brake. The drum shaft is driven by the gear reducer which power originates from a DC or AC-VF motor.

2.3.2 Hookload Sensor

A hookload sensor measures the weight that is carried by the traveling block. The reading varies in accordance with the location that the sensor is installed. In case if the sensor is mounted close to the deadline anchor, then hookload readings indicate the sum of weight of hook, traveling block, top drive, friction of the sheaves and the weight carried by the hook. In case if the sensor is mounted at the top drive, the measurements represent the weight hanging off the hook alone.

2.3.3 Travelling Block Sensor

A travelling block sensor, also known as a block position sensor, measures the distance between the travelling block and the rig floor. Usually this sensor can be mounted at the draw-works and counts the revolutions of the draw-works drum per unit time. The number of revolutions is multiplied by the circumference of the draw-works drum plus the layers of drilling line on the drum to find the travelling block movement.

2.4 Circulating System

The principle components of the mud circulation system are: mud pumps, flow lines, drill pipe, nozzles, mud mixing equipment, mud pits and tanks (mixing tank, suction tank, and settling tank) as shown in Figure 5.

The flow path of the drilling fluid, that is called mud, can be described as from the mud pit to suction line and to the pumps. At the pump the mud is pressured up and pumped through the stand pipe, the rotary rose, via the swivel into the drill string. The mud circulates through the drilling bit as it cuts through rock. The fluid lubricates the bit, removes rock cuttings, stabilizes the wellbore wall, and controls the pressure in the wellbore. The mud then from the bottom of the well rises up the annulus to the mud cleaning system that consists of shale shaker, settlement tank, desander and desilter. After cleaning the mud, the circulation circle is closed when the mud returns to the mud pit.

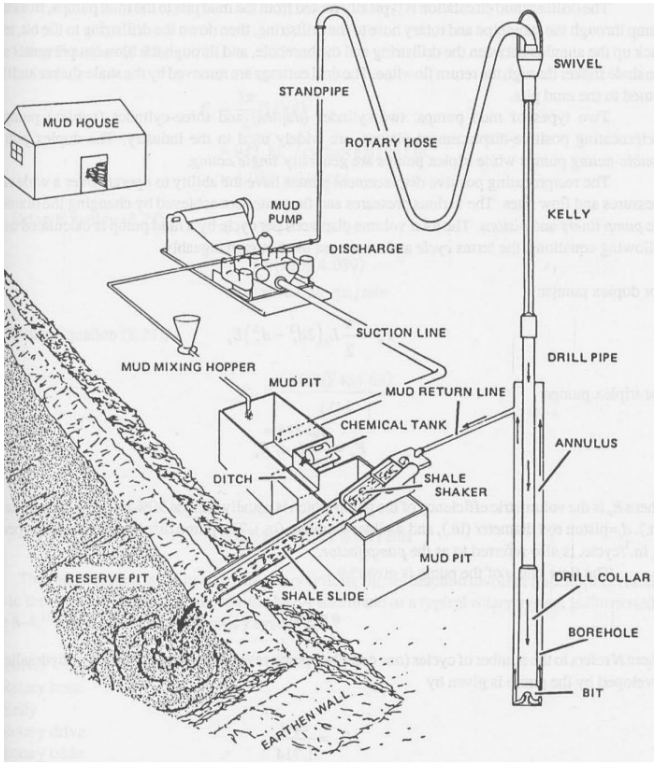

Figure 5: Circulation system (Source: Prassl, 2002).

2.4.1 Mud Pumps

The mud pumps are large pumps used to move drilling fluid through the well bore when performing drilling operation. The pump circulates the mud by pushing it down into the hole through the drill string, and then moving it back up again, through the annulus. Mud pumps are axial reciprocating piston pumps, meaning that they use oscillating pistons to displace the fluid (see Figure 6).

Figure 6: Triplex mud pumps (Source: NOV, 2014).

The mud pump is an axial piston pump that moves the fluid in only one direction. The power end converts the rotation of the motor through the drive shaft to the reciprocating motion of the axial pistons. In most cases a cross head crank gear is used for this.

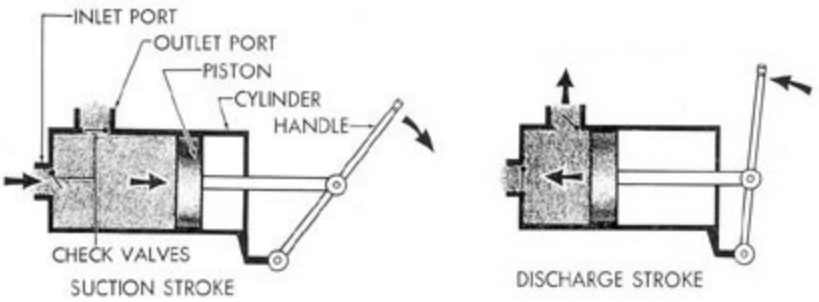

Figure 7: Single acting piston schematic (Source: GlobalSpec Inc., 2013).

There are two main parameters to measure the performance of a Mud Pump: Displacement and Pressure. Displacement is measured as discharged liters per minute. In order to remove all the cuttings from the hole and prevent settling and dropouts, a certain fluid velocity is required depending on the size of the cuttings and the viscosity of the drilling fluid. The larger the diameter of the drilling hole, the larger the necessity of displacement. The required annular fluid velocity is generally in the range of 0.4 to 1.0 m/min.

To move the drilling fluid a pressure is required to overcome the frictional forces along the drill pipe and the annulus of the hole. The deeper the well the greater the resulting pipeline resistance, the higher the pressure required.

In the Mud Pump mechanism, the gearbox or hydraulic motor is equipped to adjust its pressure and displacement to accommodate for the changing displacement requirements during drilling. To this end, a flowmeter and a pressure gauge are installed in the Mud Pump. Most modern mud pumps are triplex-style pumps, which have three cylinders. The triplex

pumps are generally lighter and more compact than the older duplex pumps and their output pressure pulsations are not as large. The overall efficiency of a triplex mud pump is the product of the mechanical and the volumetric efficiency. The mechanical efficiency is often assumed to be 90% and is related to the efficiency of the prime mover itself and the linkage to the pump drive shaft. The volumetric efficiency of a mud pump with adequately charged suction system can be as high as 100%. Therefore most manufactures rate their pumps with a total efficiency of 90% (Prassl, 2002).

2.4.2 Flow Rate Sensor

Flow rate (In): one of the most common methods of measuring the flow through an axial piston pump is to count the strokes over time and calculate the volume of each stroke. Accuracy of this flow meter is within 0.2-0.3% of the reading value (Singh, 2003).

Flow rate (Out): there are different sensors in use for this measurement, and it is common that the readings of flow rate out of these sensors vary from accurate to non-accurate results depending on the technology used. One of the most common technologies is the use of a flow paddle positioned in the flow line between the well and the shakers, which provide not accurate results since the wear of the paddles generates an error. Once high accurate data is necessary the technology used is the Coriolis type sensors. Coriolis sensors are classified as multivariable, as they provide a measurement of mass and volume flow rate, density and temperature. The mass flow rate accuracy is ±0.5% of rate at the best operating conditions. The sensor consists of a manifold which splits the fluid flow into two, and directs it through each of the two flow tubes and back out the outlet side of the manifold (Al-Morakhi, et al., 2013).

2.4.3 Pump Pressure Sensor

Surface pressure sensors are usually located close to the pump and the reading is done by the use of a diaphragm to isolate the mud from a gauges hydraulic fluid. For electrical sensors, a transducer may have a diaphragm separating the mud from an electronic strain gauge package, or the mud may act directly on the transducers steel bulkhead.

2.4.4 Mud Density Sensor

Density sensors do not always provide rapid and accurate measurements of drilling fluid density. The density sensor is also used to monitor the addition of weighting material or fluid to the mud system. Mud density is measured by two pressure sensors immersed at different depths in the mud pit. Thus, mud density is calculated from the pressure differential and depth between the sensors (Schlumberger, 2012).

2.5 Power System

The power system of a drilling rig has to supply the following main components: rotary system, hoisting system, and circulation system. In addition, auxiliaries like the blowout preventer, boiler-feed water pumps, rig lighting system, among others have to be powered. Since the largest power consumers on a drilling rig are the rotary, hoisting and the circulation system, these components determine the total power requirements.

In the past, in ordinary drilling operations, the hoisting (lifting and lowering of the drill string, casings, among others) and the circulation system were not operated at the same time. Therefore the same engines were engaged to perform both functions. But in today's drilling operations, due to the increasing complexity of the wells to be drill, the hoisting and the circulating system have to be operated at the same time (e.g. back reaming operations). Therefore the drilling rig power system must be able to provide sufficient power for all the equipment at the same time.

The power can be obtained mainly in two ways: (1) generated at the rig site using internal-combustion diesel engines or gas turbines – depending of the availability of each fuel; or (2) taken as electric power supply from existing power lines. As a guideline, the generated power at the rig site is supplied with three/four engine/generator sets, each engine has a power output between 1000 and 2000 [hp] (Prassl, 2002). The raw power is then transmitted to the operating equipment via mechanical drives, DC or AC applying a variable frequency drive (VFD). As mentioned before in Section 2, most of the newer rigs using the AC VFD systems. The model developed in this work can only be utilized for these types of rig.

The rig power system's performance is characterized by the output horsepower, torque and fuel consumption for various engine speeds. The following section provides a more detailed description of the diesel generator and the fuel consumption for the different engine speeds. Section 2.5.2 describes the working principles, design characteristics, and equipment efficiencies of the VFD system.

2.5.1 Diesel Generator

A diesel generator is the combination of two parts, a diesel engine and an electric generator, to generate electrical energy. The first part, the diesel engine, works the same as any normal internal combustion piston engine. It has an output shaft attached to the crank (the same as any car engine) which is connected to the electric generator. The second part, the electric generator, is a large alternator. The shaft of the alternator is driven by the diesel engine. Thus, the diesel engine burns fuel (diesel) to rotate the generator shaft and produce electrical energy.

Today, the majority of the new oil and gas drill rigs are AC electric rigs with VFD controls. These rigs use multiple diesel-electric generator sets running in parallel to produce the two to

four MW of power needed at the drill site, including the power needed for camp loads such as lighting, heating and air conditioning for crew quarters.

Power is generated as AC and then directly connects with the VFD room. The VFD unit allows precise control of the flow of power to any of the rig's AC motor loads while the generators running at a constant speed (load).

The number of generators needed by a rig varies with the depth of the drilling operation, but today drillers have to go deeper vertically and sometimes just as far horizontally, and that requires more power. Generator sets can easily be added to the AC powered rig to match the power requirements, making this design the most flexible. The number of generator sets running at the same time can be varied, depending on total load and fuel saving. This configuration is also more reliable because a failure of one of the generator sets does not necessarily cause a shutdown of drilling operations even though it may reduce the total amount of power available. An additional advantage of paralleled generator sets is that individual units can be taken offline for maintenance without greatly affecting the drilling operation.

Fuel Consumption

Since drilling rig generator sets operate continuously, fuel consumption accounts for the largest operational cost. Just a few percentage points of better fuel economy can add a significant number of dollars to the bottom line at the completion of a well. Diesel engines tend to be most fuel-efficient in proportion to their output when operated at 100 percent of their rated load. Engines are typically rated in terms of their brake specific fuel consumption (BSFC), which varies with the percentage of rated load. The BSFC rating allows comparing the fuel economy of generator sets before the units are in the field. For 1,200-rpm generators sets with a rating of about 1,100 kW, the BSFC should be less than 200 grams of fuel per kWh generated. For maximum fuel economy it is recommended to always operate the generator sets as near their nameplate rating as possible.

The fuel consumption of a generator changes as the elevation above mean sea level changes. With the increase of the height there is power loss due to reduction in air mass flow and poor combustion efficiency due to change in the resulting injection characteristics. The power output of diesel engines falls at the rate of about one per cent for every 100 m altitude (Sivasankaran & Jain, 1988).

The table below approximates the fuel consumption of a diesel generator based on the size of the generator and the load at which the generator is operating. Please, note that this table is intended as an estimation of how much fuel a generator uses during operation and it is not an exact representation due to various factors that can increase or decrease the amount of fuel consumed.

Table 1: Fuel Efficiency Consumption Table

Generator Size (kW)	Full Load (gal/hr)	3/4 Load (%)	1/2 Load (%)	1/4 Load (%)
20	1.6	81.3%	56.3%	37.5%
30	2.9	82.8%	62.1%	44.8%
40	4	80.0%	57.5%	40.0%
60	4.8	79.2%	60.4%	37.5%
75	6.1	75.4%	55.7%	39.3%
100	7.4	78.4%	55.4%	35.1%
125	9.1	78.0%	54.9%	34.1%
135	9.8	77.6%	55.1%	33.7%
150	10.9	77.1%	54.1%	33.0%
175	12.7	76.4%	53.5%	32.3%
200	14.4	76.4%	53.5%	32.6%
230	16.6	75.3%	53.0%	31.9%
250	18	75.6%	52.8%	31.7%
300	21.5	74.9%	52.6%	31.6%
350	25.1	74.5%	52.2%	31.5%
400	28.6	74.5%	52.1%	31.1%
500	35.7	73.9%	51.8%	30.8%
600	42.8	73.6%	51.4%	30.8%
750	53.4	73.6%	51.3%	30.5%
1000	71.1	73.3%	51.2%	30.4%
1250	88.8	73.2%	51.0%	30.3%
1500	106.5	73.1%	51.0%	30.2%
1750	124.2	73.0%	50.9%	30.2%
2000	141.9	72.9%	50.9%	30.2%
2250	159.6	72.9%	50.8%	30.1%

(Source: modified from Diesel Service & Supply, 2013)

2.5.2 Variable Frequency Driver (VFD) Room

The VFD room accommodates all the necessary equipment to provide smooth, reliable, and safe distribution of power to all AC motors on the drilling rig. The room is fully enclosed, weather proof, fully insulated and air-conditioned. The key technology used for adjusting motor, voltage and frequency to deliver only and precisely the required torque and speed is an electronic controller VFD (Figure 8). This independent component connects the generator set and the AC motors as consumers (e.g. top drive, draw-works, and mud pump).

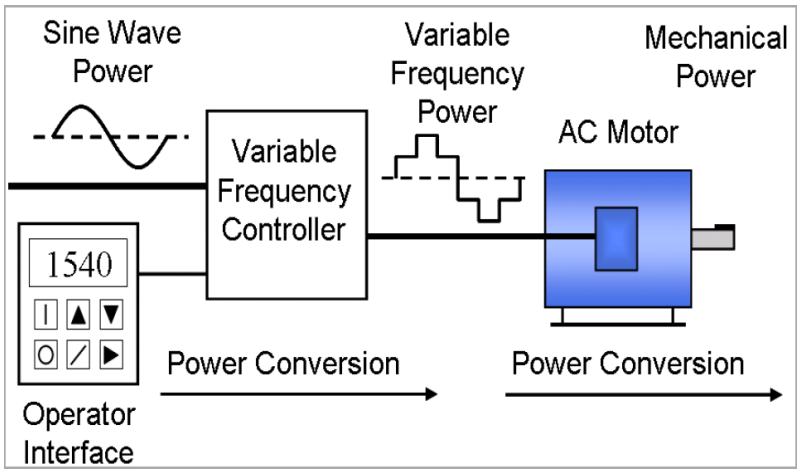

Figure 8: Schematic variable-frequency drive (Wikipedia, 2013).

The VFD usual design is first converts AC input power to DC intermediate power using a rectifier or converter bridge. The rectifier is usually a three-phase, full-wave-diode bridge. The DC intermediate power is then converted to quasi-sinusoidal AC power using an inverter switching circuit. The inverter circuit is probably the most important section of the VFD, changing DC energy into three channels of AC energy that can be used by an AC motor. These units provide an improved power factor, less harmonic distortion, and low sensitivity to the incoming phase sequencing than older phase controlled converter VFD's. The VFD is mostly based on pulse width modulation. It has power demand in both standby and subsequent variable operational modes, so additional losses of a VFD have to be over compensated by reducing losses in partial load.

Many of the new motor technologies operate with variable speeds. This means that they electronically adapt the speed rather than being based on a fixed speed design with 2, 4, 6 or 8 poles. Advanced adjustable speed controllers offer several advantages (Waide & Brunner, 2011):

- They can eliminate the major source of partial-load losses, such as mechanical resistance elements (throttles, dampers, bypasses).
- Adjustable speed and torque systems can be used for direct drive, eliminating unnecessary components such as gears, transmissions and clutches, and reducing cost and losses.
- Maintenance costs can be lowered, since lower operating speeds result in longer life for bearings and motors.
- A soft starter for motor is no longer required.
- Ability of a VFD to limit torque to a user-selected level can protect drive-equipment that cannot tolerate excessive torque.

AC motor characteristics require the applied voltage to be proportionally adjusted whenever the frequency is changed in order to deliver the rated torque. For example, if a motor is designed to operate at 460 volts at 60 Hz, the applied voltage must be reduced to 230 volts when the frequency is reduced to 30 Hz. Thus the ratio of volts per hertz must be regulated

to a constant value (460/60 = 7.67 V/Hz in this case). For optimum performance, some further voltage adjustment may be necessary especially at low speeds, but constant ratio of volts per hertz is a general rule. This ratio can be changed in order to change the torque delivered by the motor (Automation Consulting, LLC, 2011).

In addition to this simple volts-per-hertz control more advanced control methods such as vector control and direct torque control (DTC) exist. These methods adjust the motor voltage in such a way that the magnetic flux and mechanical torque of the motor can be precisely controlled

VFDs consume energy within their control circuits (motor control, network connection, input/output [I/O] logic controllers, etc.) and lose energy, particularly in the output switches. The losses of these inverters are relatively low and their efficiency in partial load is typically better than cage induction motors. VFDs also induce further losses in the motor due to harmonic distortion and non-sinusoidal output-voltage waveform. The main influencing factors on total losses are the switching frequency and the output current (which is basically associated with output power and load). Waide & Brunner (2011) presents the variable frequency drive efficiencies for different VFD nominal output power and motor loads (Figure 9).

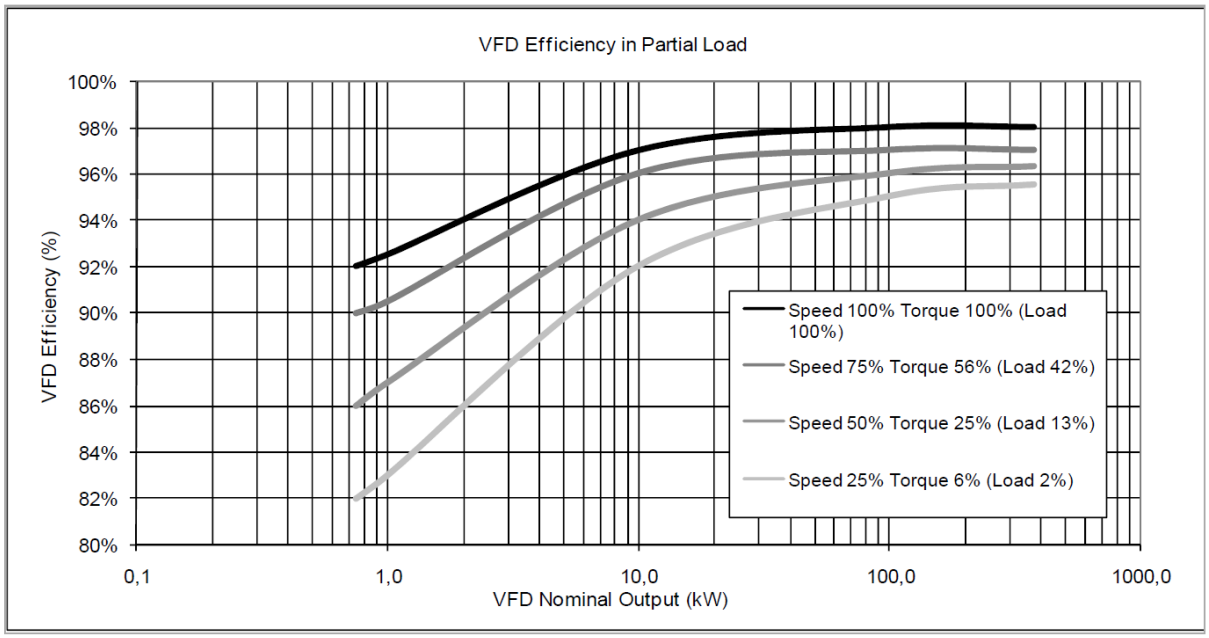

Figure 9: VFD efficiency at full and partial load. (Source: Waide& Brunner, 2011)

2.6 Other Rig Sensors

This section presents readings that can be calculated with the help of other sensors.

2.6.1 Hole Depth Readings

Hole Depth reading provides the depth of the hole drilled. It is a calculated channel based on Bit Depth Readings (see next) and typically reflects the largest bit depth reached at any point in time. This measurement usually requires manual resets and is prone to errors based on that.

2.6.2 Bit Depth Readings

Bit Depth is typically a distance between a surface reference point (e.g. rotary kelly bushing) and the bit location in the hole. These readings help the driller determine the location of the drill bit in the wellbore. It is a calculated channel based on the Block Height readings and the drill string pipe tally sheet.

2.6.3 Weight on Bit Readings

Weight on Bit (WOB) is calculated by subtracting the theoretical weight of drill string from hookload measurements while the bit is on bottom. These readings help the driller to estimate how much weight is applied on the drill bit. There is no WOB while tripping operations, since the bit is not on the bottom of the hole. The measurement typically does not consider friction in the form of drag. Thus for inclined or horizontal wells the WOB will reflect a wrong number.

3. Energy Consumption Mathematical Model

A quantitative description of a physical process always requires a mathematical formulation. These mathematics aim at approximating the process in the best possible wayand refer to the most important aspects. These mathematics are summarized by the term mathematical model (Heinemann, 2005).

This chapter describes the mathematical model that was created to simulate the energy consumption of a drilling rig. Any system properties, which are not included in the mathematical model cannot be taken into consideration for further calculations.

Drilling rigs are equipped with several electricity consuming components. To calculate the energy consumption of a drilling rig, it is necessary to calculate energy consumed by each component. Thus, the model created in this thesis simulates each of these three main components, which are: top drive, mud pumps and draw-works. The remaining part of the energy consumed by all the other extra equipment on the rig is also included into the model in a more simplified way.

For a coherent description of the developed model, this chapter is divided into three sections. The first section defines all input data, which are necessary to run the model. The second section explains necessary concepts (e.g. energy, power, efficiencies) and equations used to develop the model. The third section deals with each component used for mathematical model and describes them particularly. The third section is divided into five sub-sections. The first four subsections present a detailed description of the steps taken to calculate the total electrical power requirements for each of the four sub-models (i.e. top drive, mud pumps, draw-works, and extra equipment). The last sub-section presents an integration of the four sub-models into one final result of total energy required per unit of time.

3.1 Input Data

The process of mathematical model development aims to combine both, accuracy in the results and least amount of data to run the model. The requirement of least data is essential for many oil companies, which are limited in terms of gathering and sharing information with the third parties. Thus, a complicated model that requires a lot of inputs to run is not in demand based on the research and market investigation of the company supporting this thesis.

As result of the research, the following information was chosen to be used as input to run the model:

- Drilling data channels (Date; Time; Block Height; Hookload; Top Drive RPM; Top Drive Torque; Flow In Rate; Pressure Pump; Mud Weight);

- Specification of the rig equipment (mud pumps, draw-works, top drive, VFD room, other equipment).

The flow chart below presents a simple visualization of the suggested model.

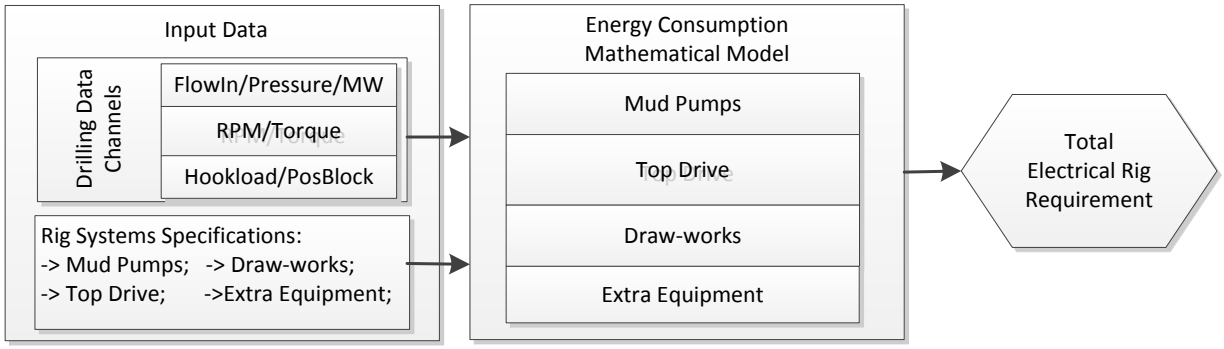

Figure 10: Energy consumption model flow chart.

3.1.1 Drilling Data Channels

The drilling data channels reflect the information recorded by rig sensors. This information is gathered in real time and transmitted via WITSML to a data base, where it is stored. Drilling data can have different sampling frequencies and is specified by a mud logging company collecting the data set. Table 2 presents the name, dimension, and units from the drilling data channel used in this thesis.

Table 2: Minimum set of data channels.

Channel	Dimension	Unit
Block Height	length	m
Flow In Rate	volumeover time	m^3/h
Hookload	weight	kg
Top Drive RPM	1 over time	rpm
Top Drive Torque	forcebylength	N.m
Pressure Pump	pressure	Pa
MudWeight	weightovervolume	kg/m^3

Table 3 depicts the drilling data channels that are used as input information for the model and also presents one minute of real drilling data. Further, this drilling data example is used as a base for several calculations and examples during the thesis. These data are collected at the sampling frequency of 0.2 Hz (sampling period of 5seconds).

Table 3: Drilling Data used in the model with 0.2 Hz sampling frequency.

Date	Time	Block Height [m]	Flow In Rate [m3/h]	Hookload [kg]	Top Drive RPM [rpm]	Top Drive Torque [N.m]	Pressure Pump [mH2O]	MudWeight [kg/m3]
14.09.2013	06:00:00	35.5	190.1	65667	68.7	2454.2	1459.1	1521.8
14.09.2013	06:00:05	35.4	206.4	65077	71.4	2118.0	1635.0	1521.8
14.09.2013	06:00:10	35.1	206.4	64442	71.4	2259.0	1639.1	1521.8
14.09.2013	06:00:15	34.8	206.4	62265	71.1	4006.8	1652.3	1521.8
14.09.2013	06:00:20	34.6	206.4	58500	71.0	6142.4	1725.3	1521.8
14.09.2013	06:00:25	34.4	206.4	58817	71.0	6378.3	1735.7	1521.8
14.09.2013	06:00:30	34.2	206.4	58817	71.3	5844.1	1737.3	1521.8
14.09.2013	06:00:35	34.0	206.4	58863	71.4	5732.9	1739.0	1521.8
14.09.2013	06:00:40	33.8	206.4	58681	71.4	5768.1	1737.1	1521.8
14.09.2013	06:00:45	33.6	206.4	58409	71.4	5917.3	1793.2	1521.8
14.09.2013	06:00:50	33.3	206.4	56640	71.1	7578.3	1855.7	1521.8
14.09.2013	06:00:55	33.0	206.4	53783	71.2	8470.5	1896.9	1521.8
14.09.2013	06:01:00	32.7	206.4	52830	71.4	8886.8	1929.8	1521.8

The frequency of 0.2 Hz was chosen as input in the mathematical model because of two main reasons. The first is that sampling frequency smaller than 0.2 Hz does not represent the dynamic behavior of operations of the rig correctly. Thus the results collected with this frequency would be wrong. The second reason is that the drilling data usually is provided via WITSML protocol, which has a sampling frequency of 0.1 - 0.2 Hz.

There are two ways to obtain necessary drilling data in order to run the Energy Consumption Mathematical Model. The first option is to access real drilling data. For that it is necessary to have authorization. Once the authorizations are granted, the data base can be accessed via web and necessary drilling data to run the model can be downloaded. The second option is to use the Drilling Data Simulator to generate the drilling data based on the pre-defined well plan.

3.1.1.1 Drilling Data Quality Control

The drilling data channels may contain problems from different sources such as: physically damaged sensors, incorrectly calculated data channel, wrong sensor calibration, among others. Thus, a quality control of the data should be performed before the data is used. The following list represents the quality control health checks that can be performed to evaluate data quality: validity, accuracy, consistency, integrity, timeliness, completeness and continuity (Arnaout, Zoellner, Johnstone, & Thonhauser, 2013).

Quality management analysis of the data channels was developed in order to assure the quality of the input data used in the model. The two main quality management steps, which

are used in this thesis, are data standardization and data quality control as proposed in (Mathis & Thonhauser, 2007).

Data Standardization

Data standardization is the first and the most crucial step in quality management analysis. Different problems need to be analyzed to assure data quality. The problems analyzed in this thesis are:

- Unit definition – to use the data, the units of the measurements needs to be defined to ensure the correct transformation to the units used by the model;
- Null values–a null value is a value used to signify that a specific value does not have a valid measurement. The value used in practice is -999.25. The null value needs to be standardized to allow the correct treatment of this data before it is used by the model;
- Time stamping and time zones – the use of a standardized data and time.

Data Quality Control

Data quality control from this thesis consists of the following steps:

- Range check – simple analysis if the range of the channels fits the model. This is based on the frequency that the data is sampled. In this thesis a period of 24 hours is used;
- Null values filling – all the null values in the data are replaced for the value of zero. Thus, the null values do not influence the final results;
- Outlier removal – this analysis removes unrealistic values from the data based on cut-off created with the use of the rig system specifications.

All the steps above are performed automatically to facilitate the use of the model.

Rig Systems Specifications

The specification of the rig equipment is obtained from the manufactures of the equipment. The main necessary information includes equipment power rating and efficiencies (i.e. motor efficiency for 50%, 75%, and 100% of loading and overall efficiency). Also, it is necessary to have an estimated overall value for the power consumption of all other equipment (i.e. excluding top drive, mud pumps and draw-works).This information is used as input for the mathematical model described in the following sections of the thesis. The table below shows an example of necessary information for the equipment specification.

Table 4: Top drive, mud pumps and draw-works necessary specifications.

	Top Drive	Mud Pumps		Draw-works	
Power Rating [kW]:	500	**Power Rating [kW]:**	500	**Power Rating [kW]:**	500
Top Drive Weight [kg]:	15000	**Overall Eff. [%]:**	85%	**Overall Eff. [%]:**	85%
Overall Eff. [%]:	85%			**Overall Eff. [%]:**	85%
Load	**Efficiency**	**Load**	**Efficiency**	**Load**	**Efficiency**
50%	93.50%	50%	94.90%	50%	94.50%
75%	94.70%	75%	95.20%	75%	94.10%
100%	95.10%	100%	94.80%	100%	93.20%

3.2 General Energy Consumption Concepts

The total energy required by the equipment for an AC Electrical Drilling Rig is the electrical energy provided by the AC generator. All the equipment use AC current to power their motors to perform a certain work. The total energy required can be calculated by:

$$E = P_{ele} \times t \ [J] \quad \textbf{Eq. 1}$$

where:

E - Energy [J];

P_{ele} - Electrical Power [W];

t - Time [s].

The equation above defines that the consumed energy is the product of electrical power required for the equipment to perform a certain work, multiplied by the time period for which this power was required. The Joule, symbol J, is a derived unit of energy, work or amount of heat in the International System of Units.

The electrical power required by the equipment to perform some work can be calculated from:

$$P_{ele} = P_{mec\ or\ hyd} \times \eta_{overall} \times \eta_{motor} \times \eta_{VSD} [W] \quad \textbf{Eq. 2}$$

where:

$P_{mec\ or\ hyd}$ - Mechanical or Hydraulic Power [W];

$\eta_{overall}$ - Overall efficiency [%];

η_{motor} - Motor efficiency [%];

η_{VFD} - VFD efficiency [%].

A different way to present the same equation is:

$$P_{ele} = P_{mec\ or\ hyd} + \sum Losses_{Overall} + \sum Losses_{Motor} + \sum Losses_{VFD}\ [W] \quad \textbf{Eq. 3}$$

where:

$\sum \text{Losses}_{\text{Overall}}$ - Overall Losses [W];

$\sum \text{Losses}_{\text{Motor}}$ - Motor Losses [W];

$\sum \text{Losses}_{\text{VFD}}$ - VFD Losses [W].

The standard metric unit of power is the Watt (W). As it is implied by Eq. 1, a unit of power is equivalent to a unit of energy divided by a unit of time. Thus, a Watt is equivalent to a Joule/second.

For a better understanding of the equations above see Figure 11 below.

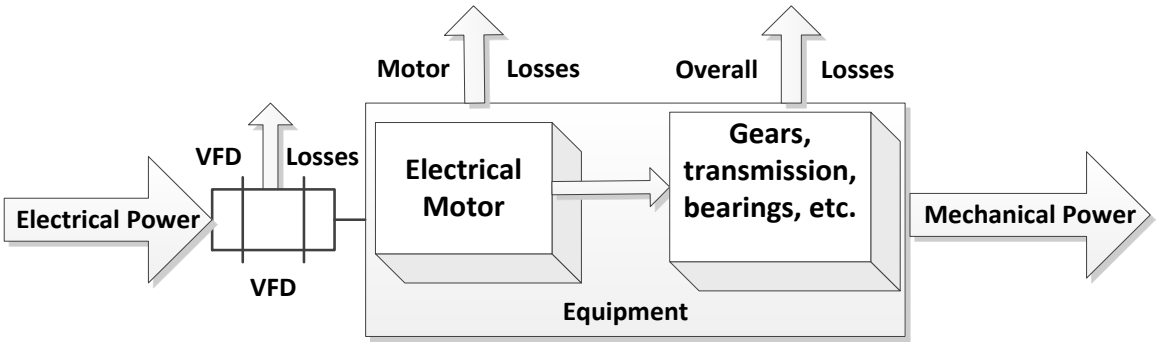

Figure 11: Energy flowin a rig equipment.

From the figure above and Eq. 3 it is possible to understand that to calculate the electrical power required (Power Input) by the equipment, firstly, it is necessary to calculate the power output (e.g. mechanical power and hydraulic power) produced by the equipment and the losses of the system (e.g. motor losses, overall losses, and VFD losses).

This section describes the concepts and equations used for calculation of the two possible power outputs: mechanical and hydraulic. Also, this section describes the concepts and equations to calculate the losses in the system: the overall, motor and VFD losses.

3.2.1 Power Output

The power output can be either mechanical power (e.g. top drive and draw-works) or hydraulic power (e.g. triplex piston axial pumps).

3.2.1.1 Mechanical Power

Mechanical power is the product of forces and movements. In particular, power is the product of a force on an object and the object's velocity, or the product of a torque on a shaft and the shaft's angular velocity.

By definition,

$$P_{mec} = f \times \frac{d}{t}[W] \quad \textbf{Eq. 4}$$

where:

f - Force [N];

d - Distance [m].

Deriving the previous equation results in:

$$P_{mec} = \frac{T \times n}{9.5492965}[W] \quad \textbf{Eq. 5}$$

where:

T - Torque [N.m];

n - Rotation [rpm].

As an example, from Eq. 5, it is possible to conclude that with the drilling data channels torque and RPM from a top drive (see Table 3) it is possible to calculate the mechanical power produced by this equipment.

3.2.1.2 Hydraulic Power

Hydraulic Power is characterized by the main variables, pressure and flow, whose product results in power. Pressure is force per unit area and flow Q is volume per time. For hydraulic calculations, the fluid is generally assumed incompressible.

By definition, the hydraulic power is calculated as:

$$P_{hyd} = \frac{P \times Q \times g \times \rho}{3.67 \times 10^{-1}}[W] \quad \textbf{Eq. 6}$$

where:

P - Pressure [Pa];

Q - Flow In [m3/h];

g - Gravity [m/s2];

ρ - Fluid density [kg/m3].

As an example, from Eq. 6, it is possible to conclude that drilling data channels pump pressure, flow-in rate and mud weight from the mud pump (see Table 3) allow to calculate the hydraulic power performed by this equipment.

.

3.2.2 System Losses and Efficiency

The efficiency can be defined as the ratio of the output power to the input power, and is usually expressed as a percentage (η is the Greek letter neta). The output power of equipment is always less than the input power because some of the energy supplied is lost (see Figure 11).The losses in machines are forms of output energy which is not used and, therefore, not desired. An electric motor converts electrical energy into mechanical energy, but also produces heat which is not desired. This heat is a loss. It means that the heat is generated, but is not used. Losses occur in all types of machines and take many forms other than heat such as sound, vibration and internal resistance. The effect of losses is the reduction of efficiency of a machine (Australian, 2008).

The general formula of efficiency is presented below:

$$\eta = \frac{P_{output}}{P_{input}} \times 100 \quad \textbf{Eq. 7}$$

where:

η - Efficiency [%];

P_{output} - Output power [W];

P_{input} - Output power [W].

Another way to represent efficiency of a system is to estimate the total losses of the system.

$$P_{ele} = P_{mec\ or\ hyd} + \sum Losses\ [W] \quad \textbf{Eq. 8}$$

where:

$\sum Losses$ - Losses [W].

Combining both equations it is possible to derive the following equation:

$$\sum Losses = \left(\frac{1}{\eta} - 1\right) \times P_{mec\ or\ hyd}[W] \quad \textbf{Eq. 9}$$

In Eq. 9 the losses of equipment are related to the efficiency of the system and output power. In this thesis the model simplifies all the losses into:

- Overall losses – fixed value related to the mechanical system to which the motor is coupled;
- Motor losses - varies according with the load of the motor;
- VFD losses – varies according with the electrical power required by the motor.

3.2.2.1 Overall Losses

As in any equipment the overall efficiency varies according with the load applied. As stated in (Azar & Samuel, 2007) and manufacture manuals (e.g. Aker Wirth and Bentec), a fixed value of efficiency is adopted to represent all energy losses (e.i. transmission, gear, bearing, friction, hydraulic, volumetric, among others).In electric motor-driven systems, additional energy losses occur in the motor itself, the section below explains these losses.

This thesis describes models of three types of equipment that are the main energy consumers in a drilling rig. Moreover, the model considers the overall losses of the systems that are related to each equipment. The overall losses are described in the respective sub-sections of the following Section 3.3, where a mathematical model for each equipment is presented.

3.2.2.2 Motor Efficiency and Losses

A motor's function is to convert electrical energy into mechanical energy to perform useful work. The only way to improve motor efficiency is to reduce motor losses. Motor energy losses can be segregated into five major areas, each of which is influenced by design and construction decisions. Motor losses may be categorized as those which are fixed, occurring whenever the motor is energized, and remaining constant for a given voltage and speed, and those which are variable and increase with the motor load (McCoy, Litman, & Douglass, 1993). These losses are described below and after summarized in the Table 5.

1. **Core loss** represents energy required to magnetize the core material (hysteresis) and includes losses due to creation of eddy currents that flow in the core. Core losses are decreased through the use of improved permeability electromagnetic (silicon) steel and by lengthening the core to reduce magnetic flux densities. Eddy current losses are decreased by using thinner steel laminations (Saidur, 2009).
2. **Friction losses** occur due to bearing friction and air resistance. Improved bearing selection, air-flow and fan design are employed to reduce these losses. In an energy-efficient motor, loss minimization results in reduced cooling requirements so a smaller fan can be used. Both core losses and friction losses are independent of motor load (Saidur, 2009).
3. **Stator losses** appear as heating due to current flow (I) through the resistance (R) of the stator winding. This is commonly referred to as an I2R loss. I2R losses can be decreased by modifying the stator slot design or by decreasing insulation thickness to increase the volume of wire in the stator (Saidur, 2009).

4. **Rotor losses** appear as I^2R heating in the rotor winding. Rotor losses can be reduced by increasing the size of the conductive bars and end rings to produce a lower resistance or by reducing the electrical current (Saidur, 2009).
5. **Stray load losses** are the result of leakage fluxes induced by load currents. Both stray load losses and stator and rotor I2R losses increase with motor load (Saidur, 2009).

Table 5: Motor loss categories

No Load Losses	Typical Losses (%)	Factors Affecting these Losses
Core Losses	15 -25	Type and quantity of magnetic material
Friction and Windage Losses	5 - 15	Selection and design of fans and bearings
Motor Operating Under Load		
Stator I^2R Losses	25 - 40	Stator conductor size
Rotor I^2R Losses	15 - 25	Rotor conductor size
Stray Load Losses	10 - 20	Manufacturing and design methods

As described above the variation of motor losses occurs due to motor loading. These losses are the same for each of the motors in a drilling rig. Thus, the description to calculate the motor losses is only presented in this section, but the calculation is performed for each of the equipment modeled in this thesis.

To calculate the motor losses firstly it is necessary to obtain from the manufacturer of the motor the efficiencies for the loads 50%, 75% and 100%. By using Eq. 9 with the loads and efficiencies of the equipment it is possible to calculate the losses for the loads 50%, 75% and 100% respectively (see Figure 12).

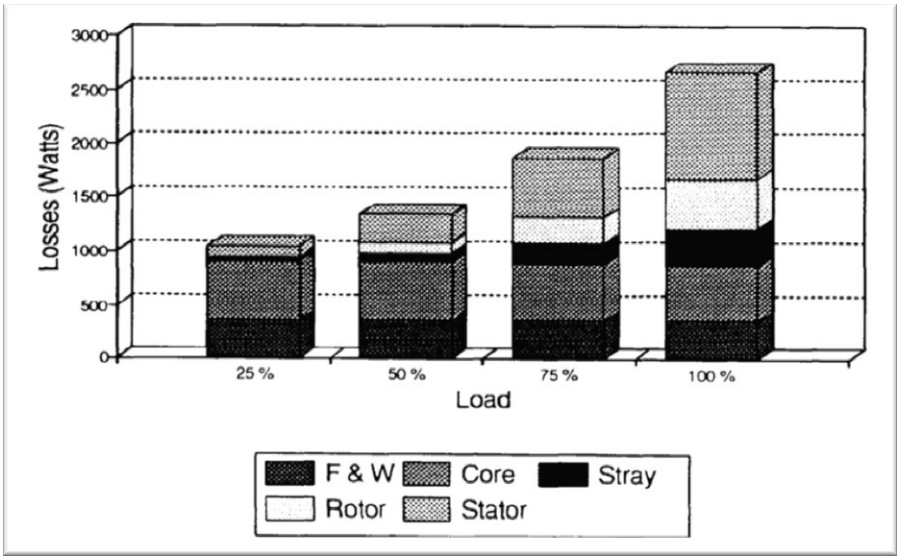

Figure 12: Variation in losses due to motor loading (Source: McCoy, Litman, & Douglass, 1993).

The losses of an engine are composed of two parts. One part is proportional to the square of the voltage (in our case considered constant) and another is proportional to the square of the current. The current is proportional to the load. Thus the losses are composed of a fixed component and a component proportional to the square of the load. A graph is created using the values of the square of the load versus the losses (see Figure 13). A regression line can be drawn to connect the points. The resulting straight line approximation (ax + b) gives the fixed component of the losses (b) and the dependence of the square of the load (a). Thus the equation representing this regression line can describe the motor losses for any load on the motor. This procedure is adopted for the three modeled equipment described in the thesis. Figure 13 shows a graphic of motor losses.

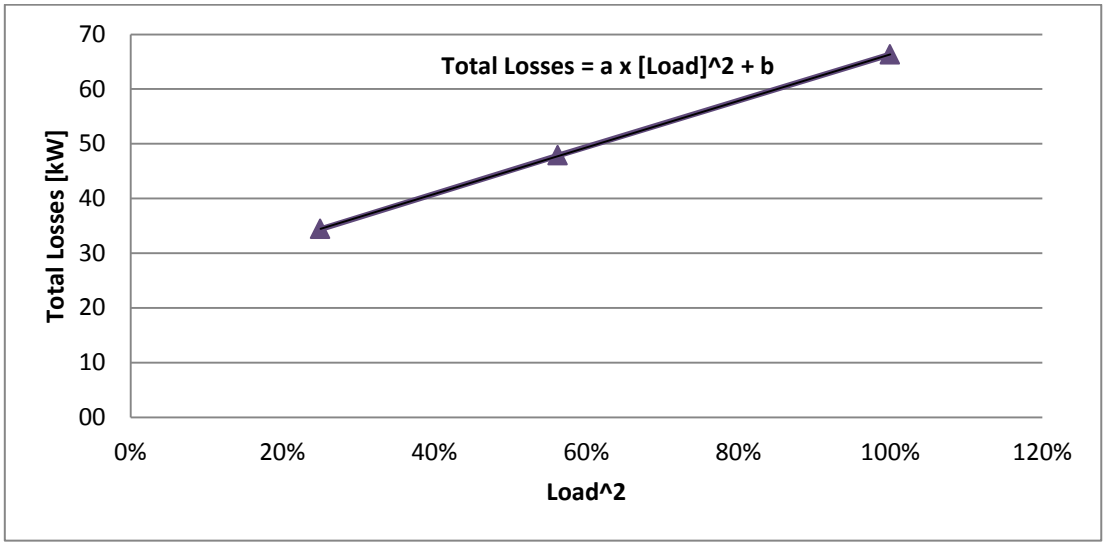

Figure 13: Motor losses by the square of the load of a top drive with the regression line.

3.2.2.3 VFD Losses

The VFD Losses calculate the energy losses of the VFD room for each equipment element. As described in Section 2.5.2, the VFD room has power demand in both standby and subsequent variable operational modes, so consequently losses vary according to the load value (Burt, Piao, Gaudi, Busch, & Taufik, 2006).

The procedure of VFD losses calculation is complicated because the manufacturer does not provide all necessary specification of the equipment for this calculation. Thus, to resolve this issue, a general equation is created to calculate the efficiency of VFD based on studies presented by Waide & Brunner (2011) and Burt et al. (2006).

$$\eta_{VFD} = 0.9385 + 0.04169 \times {P_{ELE}}^{0.3339} \left[\frac{m}{s}\right] \quad \textbf{Eq. 10}$$

The Eq. 10 created in this thesis represents the efficiency of a variable speed drive varying with the load. Such equation provides representative values of efficiencies for the equipment modeled in this thesis. Figure below is a graphical representation of Eq. 10.

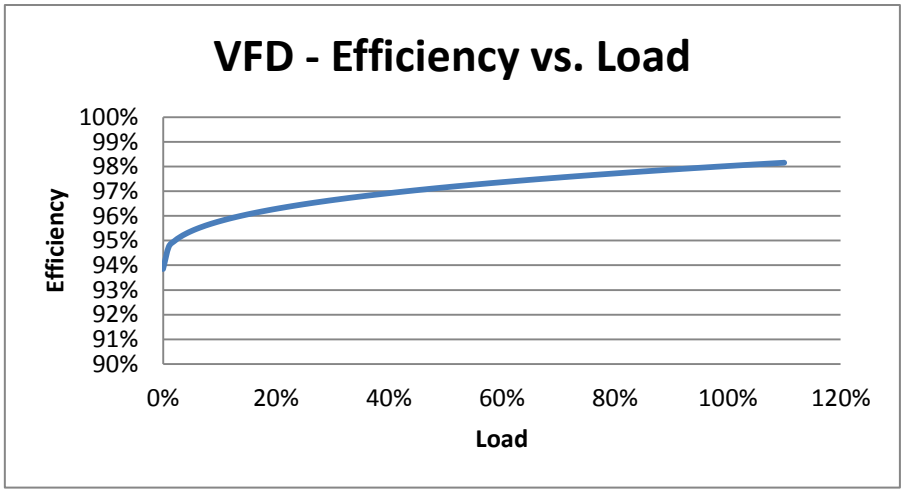

Figure 14: Graphic representation of the load vs. efficiency for the VFD.

Once the efficiency of the VFD is calculated for the corresponding load using Eq. 10, the power losses of the VFD room can be calculated for the top drive, mud pumps, or draw-works.

$$\sum Losses_{VFD} = \eta_{\boldsymbol{VFD}} \times P_{equip.}[W] \qquad \textbf{Eq. 11}$$

where:

$P_{equip.}$ - Equipment power [W].

3.3 Energy Consumption Models Description

The energy consumption model created in this thesis is divided into sub-models. There are in total four sub-models and each of them represents a different system in the drilling rig.

The sub-models that represent the three main consumers in the rig (i.e. top drive, mud pumps, draw-works) have the same procedure to calculate required electrical power. The concepts and the equations necessary to understand and calculate the electrical power are presented in Section 3.2. The procedures used in these three sub-models are:

1. Calculate the power output from the drilling data (i.e. mechanical power or hydraulic power);
2. Calculate the overall losses with the power output and overall efficiency from the rig manufacture using Eq. 9;
3. Calculate the load on the electrical motor. This can be accomplished by summing the power output and overall losses and dividing it by equipment power rating:

$$L = \frac{P_{Output} + \sum Overall\ Losses}{P_{equip.}} [\%] \quad \textbf{Eq. 12}$$

where:

L - Load [%]

4. Calculate the motor losses with the help of the regression equation created for each equipment using the procedure described in Section 3.2.2.2;
5. Calculate the VFD efficiency using Eq. 10;
6. Calculate VFD losses based on the VFD efficiency and the electrical power required by the motor (Eq. 11);
7. Calculate the total electrical power of the equipment as the sum of power output, overall losses, motor losses and VFD losses (Eq. 3).

For the last sub-model (the Other Equipment) a different methodology is used. This methodology is presented in the respective section of the sub-model.

3.3.1 Top Drive Energy Consumption Model

As presented in Section 2.1, the top drive has the same working principle as a motor, where the motor transforms electrical energy into mechanical. To be able to calculate the electrical energy consumption of the top drive it is necessary to calculate the mechanical power at the shaft, overall losses, motor losses, and VFD losses (see Figure 15).

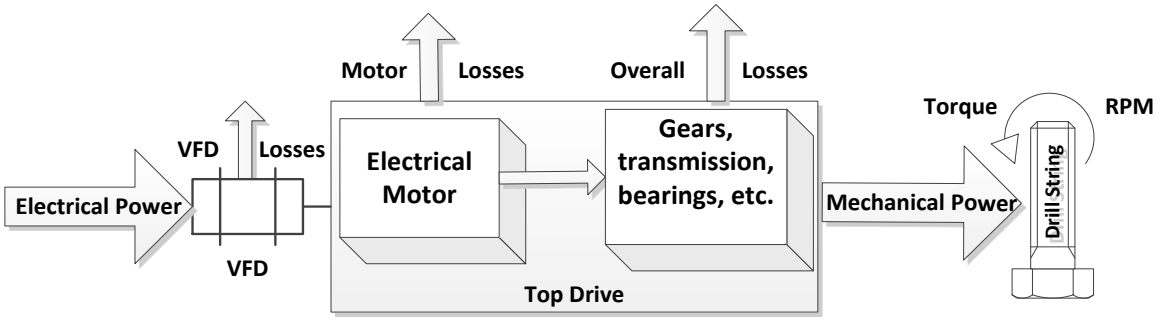

Figure 15: Energy flow in a top drive.

First, from the drilling data channels of torque and RPM it is possible to calculate the mechanical power (Eq. 5). With the calculated mechanical power and overall efficiency (provided by the rig manufacture) it is possible to calculate the overall losses using Eq. 9.The second step is to calculate the motor losses. So, based on the procedures described in Section 3.2.2.2 with the motor efficiencies for 50%, 75%, and 100% it is possible to calculate the motor losses.

The electrical power required by the motor of the top drive is given by the sum of mechanical power, overall losses and motor losses. With the electrical power required by the motor it is possible to calculate the VFD losses using Eq. 10 and Eq. 11.

The total electrical power of the equipment is the sum of power output (mechanical power), overall losses, motor losses, and VFD losses (Eq. 13).To calculate the energy consumption of the top drive it is necessary to multiply the total electrical power of the equipment by the time that the equipment required this power (Eq. 1).

$$P_{TopDrive} = P_{mec} + \sum Losses_{Overall} + \sum Losses_{Motor} + \sum Losses_{VFD}\ [W] \quad \textbf{Eq. 13}$$

where:

$P_{Top\ Drive}$ - Top drive power [W].

Table 6 presents the continuation of Table 3 which contains drilling data channels with a sampling frequency of 0.2 Hz. Table 6 presents the calculations referent to the top drive. It calculates the mechanical power performed by the top drive based on the drilling data channels top drive torque and top drive RPM presented in Table 3. Then, the overall losses, motor losses, VFD losses and total electrical power required by the top drive are calculated for 5s interval (referring to 0.2 Hz frequency) of the drilling data.

Table 6: Top drive calculation results used in the model with 0.2 Hz sampling frequency.

Date	Time	Mechanical Power [kW]	∑ Overall Losses [kW]	∑ Motor Losses [kW]	∑ VFD Losses [kW]	Total Electrical Power [kW]
14.09.2013	06:00:00	17.7	3.1	14.65	1.64	37.1
14.09.2013	06:00:05	15.8	2.8	14.65	1.55	34.8
14.09.2013	06:00:10	16.9	3.0	14.65	1.60	36.1
14.09.2013	06:00:15	29.8	5.3	14.69	2.19	52.0
14.09.2013	06:00:20	45.7	8.1	14.76	2.86	71.3
14.09.2013	06:00:25	47.4	8.4	14.77	2.93	73.5
14.09.2013	06:00:30	43.6	7.7	14.75	2.77	68.9
14.09.2013	06:00:35	42.9	7.6	14.75	2.74	67.9
14.09.2013	06:00:40	43.1	7.6	14.75	2.75	68.2
14.09.2013	06:00:45	44.2	7.8	14.75	2.80	69.6
14.09.2013	06:00:50	56.4	10.0	14.83	3.28	84.5
14.09.2013	06:00:55	63.2	11.1	14.88	3.53	92.7
14.09.2013	06:01:00	66.4	11.7	14.91	3.65	96.7

3.3.1.1 Top Drive Overall Efficiency

The adopted top drive overall efficiency is a fixed value that represents the efficiency for the rotary system (described in Section 2.2). This value estimation is based on the specification of the equipment that considers all energy losses (e.g. transmission, gear, bearing, friction) occurring in the rotary system.

Based on technical information for top drives from the company Aker Wirth it is possible to estimate the top drive overall efficiency in the range of 80-90%. If it is not possible to obtain this information from the top drive manufacturer, values can be assumed in the proposed range.

3.3.2 Mud Pumps Energy Consumption Model

As mentioned in Section 2.4.1, the mud pumps are the triplex-single acting pumps. An electrical motor provides mechanical energy for the axial-pistons to pump the drilling fluid. The pump transforms electrical energy into hydraulic energy (Figure 16).

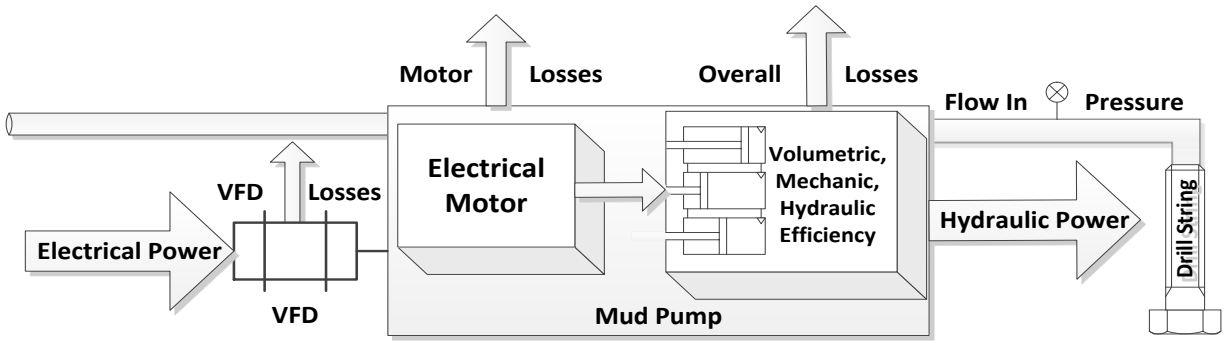

Figure 16: Energy flow in a mud pump.

To calculate the electrical energy consumption of the mud pump it is necessary to calculate the hydraulic power, overall losses, motor losses and VFD losses.

At first, from the drilling data channels of flow in, pressure and mud weight, it is possible to calculate the hydraulic power (Eq.Eq. **6**). With the calculated hydraulic power and overall efficiency provided by the rig manufacture, it is possible to calculate the overall losses using Eq. 9.The next step is to calculate the motor losses. So, based on the procedures described in Section 3.2.2.2 with the motor efficiencies for 50%, 75% and 100% it is possible to calculate the motor losses.

The electrical power required by the motor of the mud pump is given by the sum of hydraulic power, overall losses and motor losses. With the known required electrical power it is possible to calculate the VFD losses using Eq. 10 and Eq. 11.

The total electrical power of the equipment is the sum of power output (hydraulic power), overall losses, motor losses and VFD losses (Eq. 3). To calculate the energy consumption of

the mud pump, it is necessary to multiply the total electrical power of the equipment by the time that the equipment required this power (Eq. 1).

$$P_{MudPumps} = P_{hyd} + \sum Losses_{Overall} + \sum Losses_{Motor} + \sum Losses_{VFD}\ [W] \quad \textbf{Eq. 14}$$

where:

$P_{Mud\ Pumps}$ - Mud Pumps power [W]

Table 7 is the continuation of Table 3 which contains drilling data channels with a sampling frequency of 0.2 Hz. Table 7 presents the calculations referent to the mud pumps. It calculates the hydraulic power performed by the mud pumps based on the drilling data channels Flow-In Rate, Pump Pressure, and Mud Weight presented in Table 3. Then, the overall losses, motor losses, VFD losses and total electrical power required by the mud pumps are calculated for the 5s interval (corresponding to 0.2 Hz frequency) of the drilling data.

Table 7: Mud pump calculation results used in the model with 0.2 Hz sampling frequency.

Date	Time	Hydraulic Power [kW]	∑ Overall Losses [kW]	∑ Motor Losses [kW]	∑ VFD Losses [kW]	Total Electrical Power [kW]
14.09.2013	06:00:00	1150.1	171.9	64.34	38.16	1424.5
14.09.2013	06:00:05	1399.7	209.1	76.62	42.24	1727.7
14.09.2013	06:00:10	1403.2	209.7	76.81	42.29	1732.0
14.09.2013	06:00:15	1414.4	211.4	77.42	42.46	1745.7
14.09.2013	06:00:20	1476.9	220.7	80.91	43.32	1821.8
14.09.2013	06:00:25	1485.9	222.0	81.43	43.44	1832.8
14.09.2013	06:00:30	1487.2	222.2	81.50	43.46	1834.4
14.09.2013	06:00:35	1488.7	222.4	81.59	43.48	1836.2
14.09.2013	06:00:40	1487.1	222.2	81.49	43.46	1834.2
14.09.2013	06:00:45	1535.1	229.4	84.30	44.08	1892.8
14.09.2013	06:00:50	1588.6	237.4	87.52	44.74	1958.2
14.09.2013	06:00:55	1623.9	242.6	89.71	45.15	2001.4
14.09.2013	06:01:00	1652.0	246.9	91.49	45.47	2035.8

3.3.2.1 Mud Pump Overall Efficiency

The mud pump overall efficiency is a value that represents the efficiency for the circulating system (described in Section 2.4). It is a variable that describes all energy losses in a hydraulic system (e.g. hydraulic, mechanical, volumetric, friction), and its estimation is based on the specification of the equipment (Rajput, 1998).

Overall pump efficiency is a ratio of power actually gained by the fluid to the shaft power supplied. Overall efficiency is determined by multiplying hydraulic efficiency by mechanical efficiency by volumetric efficiency by friction efficiency.

$$\eta = \eta_m \times \eta_h \times \eta_v \times \eta_f \quad \textbf{Eq. 15}$$

where:

η_m - Mechanical efficiency;

η_h - Hydraulic efficiency;

η_v - Volumetric efficiency;

η_f - Friction efficiency.

Based on the technical information of mud pumps from the company Aker Wirth and Bentec it is possible to estimate a mud pump overall efficiency in the range of 80-90%. If it is not possible to obtain this information from the mud pumps manufacturer, values can be assumed in the proposed range.

Hydraulic Efficiency

Hydraulic loss relates to the construction of the pump, and is caused by the friction between the fluid and the walls, acceleration and retardation of the fluid and the change of the fluid flow direction.

The hydraulic efficiency can be expressed as:

$$\eta_h = \frac{\mathrm{w}}{(\mathrm{w} + \mathrm{w}_L)} \quad \textbf{Eq. 16}$$

where:

w - Specific work from the pump or fan [W];

w_L - Specific work lost due to hydraulic effects [W].

Mechanical Efficiency

Mechanical components, suchlike transmission gear and bearings, generate a mechanical loss that reduces the power transferred from the motor shaft to the pump or fan impeller.

The mechanical efficiency can be expressed as:

$$\eta_m = \frac{(\mathrm{P} - P_L)}{P} \quad \textbf{Eq. 17}$$

where:

P - Power transferred from the motor to the shaft [W];

P_L - Power lost in the transmission [W].

Volumetric Efficiency

Due to leakage of fluid between the back surface of the impeller hub plate and the casing, or through other pump components, a volumetric loss reducing the pump efficiency can occur.

The volumetric efficiency can be expressed as:

$$\eta_v = \frac{q}{(q + q_L)} \qquad \textbf{Eq. 18}$$

where:

q - Volume flow out of the pump or fan [W];

q_L - Leakage volume flow [W].

Friction Efficiency

Frictional efficiency corresponds to the pressure loss created by the fluid flowing through the flow path. It is a function of fluid properties influenced by pressure and temperature (density, viscosity, gel-strength), flow rate and the geometry of characteristic of flow path (hole size/drill string size). Frictional pressure loss affects the pump pressure because higher frictional pressure losses causes a higher pump pressure which is required to maintain the desired pump rate (DrillingFormula, 2010).

3.3.3 Draw-works Energy Consumption Model

To calculate the energy consumption for the draw-works is a complicated task. As described in Section 2.3, the draw-works has the same working principle as a motor, where the motor transforms electrical energy into mechanical.

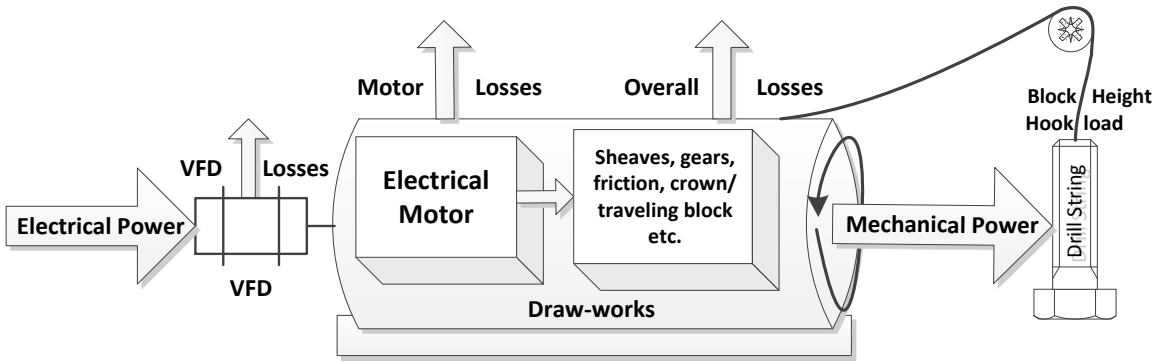

Figure 17: Energy flow in a draw-works.

The problem is that the drilling data channels do not provide the RPM and torque realized by the draw-works. Thus, the mechanical power produced by the draw-works cannot be directly

calculated. Further, studying the working principle of the hoisting system it is possible to conclude that the energy consumption for trip-in and trip-out operations should be calculated in different ways. For these reasons two different approaches are taken to calculate the energy consumption by the draw-works. One of them simulates trip-in operations and the other simulates trip-out operations. Both of them are explained in the following sections.

To understand if the rig is performing either tripping-in or tripping-out operations a simple analysis of the Block Height can be performed. If Eq. 19 has a positive result, it means that the rig is performing tripping-in operation, since the height of the block at $t + \Delta t$ is lower than at t (the drilling string is been lowered). And if Eq. 19 have a negative result, it means that the rig is performing trip out operation, since the height of the block at $t + \Delta t$ is higher than at t (the drilling string is been lifted).

$$\pm BH_t - BH_{t+\Delta t}[m] \quad \textbf{Eq. 19}$$

where:

BH - Block height [m];

Based on this analysis, the following two energy consumption models are considered in order to calculate the energy consumed by the draw-works.

3.3.3.1 Tripping-In Energy Consumption Model

The model developed for the energy consumption for tripping-in operations is based on the principles that the draw-works use only breaks when lowering the drill string. Thus only a fixed amount of power is required to activate the brakes (and not all the draw-works power is necessary).

Eq. 20shows that the break power is constant. The value to be used as input can be found in the specification of the draw-works.

$$P_{Break} = const.[W] \quad \textbf{Eq. 20}$$

where:

P_{Break} - Break power [W].

3.3.3.2 Tripping-Out Energy Consumption Model

The model developed for the energy consumption in tripping-out operations is based on the working principles of the hoisting system. After a careful analysis it is concluded that the power required by the draw-works can be calculated using the hookload and travelling block speed. In this section, the concept and mathematics used for these calculations are described.

Using the drilling data it is possible to calculate the mechanical power performed by the draw-works from the Block Height and the Hookload channels. The idea is to calculate the torque and the RPM performed by the draw-works drum based on these channels.

From the channel Block Height that describes the movement of the traveling block with respect to the rig floor it is possible to convert the difference of the block height readings into RPM of the draw-works. To achieve that, firstly, it is necessary to calculate the linear velocity of the fast line (see Eq. 21).

$$V_{linear} = \left| \frac{(BH_t - BH_{t+\Delta t})}{\Delta t} \times N_{sheaves} \right| \left[\frac{m}{s}\right] \quad \textbf{Eq. 21}$$

where:

$\mathrm{V_{linear}}$ - Fast line linear velocity [m/s];

$\Delta \mathrm{t}$ - Time difference [s];

$\mathrm{N_{sheaves}}$ - Number of sheaves .

Secondly, with the linear velocity and the drum radius of the draw-works it is possible to calculate the angular velocity of the drum.

$$\omega = \frac{V_{linear} \times 60}{2 \times \pi \times r} [\mathrm{rpm}] \quad \textbf{Eq. 22}$$

where:

ω - Angular velocity [rpm];

r - Drum radius [m].

From the channel Hookload that describes the weight carried by the hook and, consequently, by the draw-works and the drum radius, it is possible to calculate the torque.

$$\mathrm{T} = \frac{\mathrm{hk}}{N_{sheaves}} \times \mathrm{g} \times \mathrm{r}\ [N.m] \quad \textbf{Eq. 23}$$

where:

hk - Hookload [kg].

From the calculated data of Torque (Eq. 23) and RPM (Eq. 22)it is possible to calculate the mechanical power (Eq. 5). Thus, the mechanical power for the draw-works is calculated with the combination of the Eq. 21, Eq. 22, and Eq. 23. The resultant equation from the combination of those equations is presented below:

$$P_{mec} = \left| \frac{(BH_t - BH_{t+\Delta t})}{\Delta t} \right| \times \mathrm{hk} \times \mathrm{g}\ [W]. \quad \textbf{Eq. 24}$$

Analysis of the equation above leads to the conclusion that the information of number of sheaves in the crown block/traveling block and the radius of the drum is not necessary for the calculation of the mechanical power of the draw-works. This is explained by the fact that the weight of the hookload applied at the draw-work is divided by the number of sheaves; and, the same time, the draw-works speed is directly proportional to the amount of sheaves. Thus, both parameters cancel each other out. It makes the mathematical model simpler since fewer inputs are required.

With the calculated mechanical power and overall efficiency provided by the rig manufacture it is possible to calculate the overall losses using Eq. 9.The next step is to calculate the motor losses. So, based on the procedures described in Section 3.2.2.2 with the motor efficiencies for 50%, 75%, and 100% it is possible to calculate the motor losses.

The electrical power required by the motor of the draw-works is given by the sum of mechanical power, overall losses, and motor losses. With the required electrical power it is possible to calculate the VFD losses using Eq. 10 and Eq. 11.

The total electrical power of the equipment is the sum of power output, overall losses, motor losses and VFD losses (Eq. 25). To calculate the energy consumption of the draw-works, it is necessary to multiply the total electrical power of the equipment by the time that the equipment required this power (Eq. 1).

$$P_{Draw-works} = P_{mec} + \sum Losses_{Overall} + \sum Losses_{Motor} + \sum Losses_{VFD}\ [W] \quad \textbf{Eq. 25}$$

where:

$P_{Draw-works}$ - Draw-works power [W].

Table 8: Draw-works calculation results used in the model with 0.2 Hz sampling frequency.

Date	Time	Linear Vel. [m/s]	Angular Velocity [RPM]	Torque [N.m]	Mech. Power [kW]	∑ Overall Losses [kW]	∑ Motor Losses [kW]	∑ VFD Losses [kW]	Total Elec. Power [kW]
14.09.2013	06:00:00	0.16	2.1	57977.2	12.6	4.2	17.21	1.74	35.71
14.09.2013	06:00:05	0.46	6.1	57456.6	37.0	12.3	17.32	3.18	69.80
14.09.2013	06:00:10	0.40	5.3	56895.9	31.6	10.5	17.28	2.88	62.30
14.09.2013	06:00:15	0.32	4.3	54973.6	24.6	8.2	17.25	2.47	52.49
14.09.2013	06:00:20	0.33	4.4	51649.6	23.8	7.9	17.25	2.42	51.39
14.09.2013	06:00:25	0.36	4.7	51929.9	25.7	8.6	17.26	2.54	54.03
14.09.2013	06:00:30	0.32	4.2	51929.9	22.9	7.6	17.24	2.37	50.10
14.09.2013	06:00:35	0.33	4.4	51970.0	23.9	8.0	17.25	2.43	51.60
14.09.2013	06:00:40	0.33	4.3	51809.8	23.5	7.8	17.25	2.41	51.00
14.09.2013	06:00:45	0.42	5.6	51569.5	30.4	10.1	17.28	2.81	60.61
14.09.2013	06:00:50	0.54	7.1	50007.6	37.3	12.4	17.32	3.20	70.20
14.09.2013	06:00:55	0.49	6.5	47484.6	32.5	10.8	17.29	2.93	63.53
14.09.2013	06:01:00	0.51	6.8	46643.6	33.2	11.1	17.29	2.97	64.49

Table 8 is the continuation of Table 3 which contains drilling data channels with a sampling frequency of 0.2 Hz. Table 8 presents the calculations referent to the draw-works. It calculates the mechanical power performed by the draw-works based on the drilling data channels Hookload and Block Height presented in Table 3. Then, the overall losses, motor losses, VFD losses and total electrical power required by the draw-works are calculated for the 5 s interval (corresponding to 0.2 Hz frequency) of the drilling data.

3.3.3.3 Draw-works Overall Efficiency

The adopted draw-works overall efficiency is a fixed value that represents the efficiency for the hoisting system (described in Section2.3). This value estimation is based on the specification of the equipment that considers all energy losses (e.g. transmission, gear, bearing, friction) occurring in the hoisting system.

The draw-works overall efficiency value also includes the energy losses due to friction at the crown block and the traveling block. Based on technical information of draw-works from the companies Aker Wirth and Bentec it is possible to estimate the draw-works overall efficiency in the range of 75-90%. If it is not possible to obtain this information from the draw-works manufacturer, values can be assumed in the proposed range.

3.3.4 Extra Equipment Energy Consumption Model

For this part of the model a more simplistic approach is taken. This section represents all the equipment of the rig excluding the three main consumers. Chapter 2 presents a detailed description of a drilling rig and most of the components.

Extra equipment works at constant power, meaning no load variations, which leads to no big variations in energy consumption. Thus, according to the rig specification a fixed value of electrical power can be taken to represent all these extra equipment. Based on preliminary results of the energy consumption model a representative value for the electrical power required in a drilling rig was defined in the range of 5%-12% of the total power installed.

$$P_{ExtraEquip.} = P_{inst.} \times p_{Extra\ Equip.}[W] \quad \textbf{Eq. 26}$$

where:

$P_{Extra\ Equip.}$ - Extra equipment power [W];

$P_{inst.}$ - Total power installed [W];

$p_{Extra\ Equip.}$ - Extra equipment load [%].

3.3.5 Final Integrated Model

The final part of the model is the sum of all the energy consumption described in this chapter. Figure 11 represents all energy losses and energy conversions for each equipment (top drive, mud pumps, and draw-works) in a drilling rig.

The equation summing electrical power of each equipment gives the final result.

$$P_{Total} = P_{TopDrive} + P_{MudPumps} + P_{Draw-works} + P_{ExtraEquip.}[W] \quad \textbf{Eq.27}$$

where:

P_{Total} - Total electrical power [W].

From the Eq. 1, energy is the product of electrical power by the time that this power was required. Thus, the final result of total energy required is the sum presented in the equation below.

$$E = \sum_{i=t}^{24h} P_{t.Total} \times t_t. \quad \textbf{Eq. 28}$$

The procedure to calculate the total electrical power for a drilling rig includes:

1. Calculate the power output (i.e. mechanical power or hydraulic power) performed by the equipment based on the drilling data channels for the top drive, mud pumps and draw-works;
2. Calculate the overall losses based on the power output for the top drive, mud pumps and draw-works;
3. Calculate the motor losses based on the sum of power output and overall losses for the top drive, mud pumps and draw-works;
4. Calculate the VFD Losses based on the sum of power output, overall losses and motor losses for the top drive, mud pumps and draw-works;
5. Calculate the total electrical power based on the sum of power output, overall losses, motor losses and VFD losses for the top drive, mud pumps and draw-works;
6. Calculate the total electrical power for the extra equipment;
7. Calculate the total electrical power required by the rig with the sum of the total electrical power for the top drive, mud pumps, draw-works and extra equipment;
8. Calculate the total energy consumed by the rig as the product of total electrical power required by the rig multiplied by the time that this power was required.

4. Model Confirmation, Verification& Validation

Models are increasingly being used in the industry to solve problems and to support decision-making process. Thus, the users of the models and the individuals that are affected by made decisions are correctly concerned with their accuracy and credibility. These concerns are addressed through Confirmation, Verification and Validation (CV&V) of the models (Sargent, 2011).

Figure 18 presents through the use of diagram a simplistic illustration of the modeling, implementation and simulation activities (black solid lines) and the assessment activities (red dashed lines) involved in the model CV&V. This diagram is also known as the “Sargent Circle”.

In Figure 18, the Reality of Interest represents the physical system of interest. In the thesis Reality of Interest is the complete system of a drilling rig with all the components that consume or interfere in the energy consumption. To perform CV&V of the complete system, the process shown in Figure 1 needs to be repeated multiple times as the model development progresses from unit problems (e.g. top drive, draw-works) to the complete system (i.e. drilling rig).

The Mathematical Model comprises the conceptual model, mathematical equations and modeling data needed to describe the Reality of Interest. Mathematical models are all the mathematical formulations required to imitate a real world system. In the thesis the Energy Consumption Model, described in Chapter 0, is the mathematical model. Relevant physical processes occurring on a drilling rig are described in a conceptual and mathematical form.

The computer model represents the implementation of the mathematical model. It comprises of the computer program (code), conceptual and mathematical modeling assumptions, code inputs, constitutive model and inputs, grid size, solution options, and tolerances. In this thesis the implementation of the mathematical model is performed with the use of the Microsoft Excel Software. The computer model is presented through a series of tables introduced in Chapter 3.

Model CV&V is conducted with the ultimate goal of producing an accurate and credible model. The confirmation of a model starts after the mathematical model is developed. The verification and validation (V&V) of a model is done after functional specifications have been documented and computational model has been completed. The V&V process often detects errors in the model that require significant modifications and further model re-verification and re-validation. These are iterative processes that take place throughout the final part of the model development (Thacker et al., 2004). This chapter describes the process used to perform the CV&V of the model developed in this thesis.

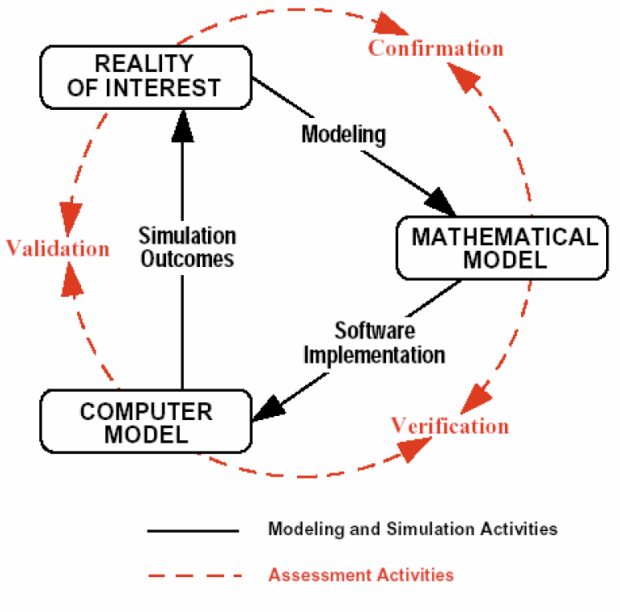

Figure 18: Simplified view of the model CV&V process (Source: Thacker, 2004).

The process of selecting important features and associated to them mathematical approximations required to represent the Reality of Interest in the mathematical model is termed as modeling (see Figure 18). Confirmation deals with assessing the correctness of the modeling. The confirmation procedure used for the model developed in this thesis is described in Section 4.1.

The verification is performed in order to assure that the created model matches specifications and assumptions with respect to the mathematics and coding. Validation checks the accuracy of the model's representation of the real system. Moreover, it quantifies uncertainties by comparing head-to-head model predictions to the real world data.

Both verification and validation are processes that accumulate evidence of a model accuracy and credibility for the specific scenarios. Thus, verification and validation cannot prove that a model is correct and accurate for all possible scenarios, but, rather, they can provide evidence that the model is sufficiently accurate for its intended use (Thacker et al., 2004).

The verification process of the model developed in this thesis is described in the following Section 4.2.The validation process of the model is more complicated. A number of steps had to be performed to achieve the desired result. A detailed description of that is provided in Section 4.3.

4.1 Model Confirmation

To assess the correctness of the developed model a simple approach is taken. The Reality of Interest and the developed Mathematical Model were taken to different specialists. Each specialist from a different field provides a specific feedback thus giving the model Confirmation.

At first, the description and assumptions of the Reality of Interest are checked by an expert to assure that it represents a Drilling Rig System correctly. With the feedback provided by the expert, some corrections are made in the assumptions of the Reality of Interest.

At second, the developed Mathematical Model is checked to assure that the conceptual model, mathematical equations, and modeling data describe the Reality of Interest correctly. This part is carried out by two experts. The first expert, Dr. Stefan Wirth (OMV) checks the model to assure that the mathematical model represents the Reality of Interest correctly in terms of the rig system functions and specifications. The second expert, Dr. Edson Bortoni (UNIFEI), checks the model to assure that each equipment (e.g. top drive, VFD) is correctly represented by the calculations, including the mechanical power performed by the equipment, the motor losses, the VFD losses, and the total electrical input power. All the necessary corrections are based on the feedback provided by the experts. After that the Mathematical Model is implemented as a Computer Model using Microsoft Excel. Once the Computer Model is ready, the verification part of the model can start.

4.2 Model Verification

Model verification is defined as “a process of determining that a model implementation accurately represents the developer’s conceptual description of the model and the solution to the model” (AIAA, 1998). In other words, it verifies if the implementation of the model is accurately accomplished in regards to codes and mathematics. Shortly, verification deals with the concepts, mathematics and codes of the model. Validation deals with the accuracy of the results of the model. As concepts, mathematical and code errors can eliminate the impression of correctness/accuracy (i.e. by giving the right answer for the wrong reason), the verification process should be realized until a high level of credibility before the validation activity begins (Thacker et al., 2004).The verification activity of the model developed in this thesis can be divided into code verification and mathematics verification.

When performing code verification, problems are devised to demonstrate that the code can compute an accurate solution. Code verification problems are constructed to verify code correctness, robustness and specific code algorithms. The purpose of code verification is to confirm that the software is working as intended. The main focus of this activity is to identify and eliminate programming and implementation errors within the software (software quality

assurance) and to verify the correctness of the numerical algorithms that are implemented in the code.

When performing mathematic verification, a model that is to be validated is exercised to demonstrate that the model is computing a sufficiently accurate solution. The purpose of calculation verification is to quantify the error of a numerical simulation (Thacker et al., 2004).

4.3 Model Validation

Model validation is defined as the "process of determining the degree to which a computer model is an accurate representation of the real world from the perspective of the intended model applications" (AIAA, 1998). It is accomplished through the comparison of predictions from a model to experimental results (Paez, 2009).

A model should be developed for a specific purpose (or application) and its validity is determined with respect to its purpose/application. In this thesis the model was developed with the application of calculating the energy consumed by a drilling rig to drill a shale gas well in Europe with the use of simulated drilling data. Thus, to validate the model it is necessary to compare the predictions of energy consumed from the model developed against experimental results of energy consumed by drilling rigs. Dedicated studies are performed to understand how it is possible to accomplish this comparison. The studies result in the comparison between the calculated values of the fuel consumed per day (based on real drilling data and the input parameters from the drilling rig) against the real values of the fuel consumed per day (obtained from the drilling morning reports). To accomplish this comparison two main steps are necessary.

Firstly, it is necessary to transform the predictions from the Energy Consumption Model into fuel consumed by the rig. This is accomplished by use of a simple mathematical model to convert the energy consumed by the rig (these are the output results of the model described in the Chapter 3) into the desired parameter. This model, called "Fuel Consumption Model", is described in the following section.

Secondly, it is necessary to obtain all necessary input data to run the models and the real values of the fuel consumed by the rig, to be able to establish a comparison between the results. This is done by using real drilling data, all the necessary specification of the equipment, and the drilling morning report from a real well. The real drilling data (in a 24h time-span form) and the equipment specification of the rig are used as input. The Energy Consumption Model provides the total energy consumed by the rig in 24 hours. Further, using Fuel Consumption Model it is possible to transform the results of energy consumed into fuel consumed by the rig in 24 hours period.

The validation may then be performed by the comparison of calculated values of daily fuel consumption against the real values of daily fuel consumptions. The comparisons and

analysis of the results for several case studies are presented and discussed in the later part of this section.

4.3.1 Fuel Consumption Model

This section describes the concepts and the mathematical formulations that are used to simulate the fuel consumption of a drilling rig. The mathematical formulation uses the total power required by the rig (output from the model described in Chapter 3) and converts it into consumed fuel. The model simulates mathematically the fuel consumption of the Diesel AC Generator on the drilling rig. The results generated by this model are presented in the Section 4.3.2 and Appendix A, where the calculated values of fuel consumption per day are compared to the real fuel consumption values per day obtained from the drilling morning reports.

For a coherent description of the developed model, this section is divided into two sub-sections. The first sub-section defines all input data, which are necessary to run the model. The second sub-section explains necessary concepts (e.g. fuel rate, fuel consumption) and equations used to develop the model. The results are presented in gal, gal/h, and gal/day because all the manufacture data, which is used as input, are obtained in these units. All the data used in the validation process of the model are obtained from USA companies, thus the fuel consumption in the morning reports are also obtained in gallons.

4.3.1.1 Input Data

The input data necessary for this model are the information regarding the generators in the rig. These data summarize all the necessary information to calculate the fuel consumption of the drilling rig. The input data are:

- Electrical rating [kW];
- Number of generators;
- Fuel consumption for different loads (0%, 25%, 50%, 75% and 100%).

The specifications of the generators for loads at 25%, 50%, 75% and 100% are obtained from the manufactures of the equipment. At No-Load (0%) the Diesel Consumption will be 10 to 10.2% of the Full Load consumption (Dhayanandhan, 2011). The table below show the input data is presented in the model.

Table 9: Generators input data.

Generator Data	
Elect. Rating [kW]	1250
Nº Generators	2
Load [%]	**Fuel Consumption [gal/h]**
100%	88.8
75%	65
50%	45.5
25%	26.9
0%	8.88

4.3.1.2 Fuel Consumption Model Description

As described in section 2.5, the generator provides all the energy consumed by the AC Electrical Drilling Rig. To accomplish that, the diesel engine burns fuel (diesel) to rotate the generator shaft and produces the electrical energy necessary to perform the job.

As described before, with the constant variation of loads, due to different operations in the drilling rig, the fuel consumption of the generator also varies. From the manufacturer of the equipment it is possible to obtain the fuel consumption for the loads 0%, 25%, 50%, 75% and 100% (used for Figure 19). Thus, the first step of the model includes calculation of the fuel consumption for any load of the generator based on the input data provided by the manufacturer.

The losses of the diesel generator are captured within the values of fuel consumption by load. The visualization of these losses is better when analyzing the fuel consumption with a load of 0% of the generators. The necessary concepts to understand the losses of the generator are presented in Section 3.2.2.

Figure 19 is a plot where load versus fuel consumption provided by the manufacturer is shown. A regression line can be drawn to connect the five points. Thus the equation representing this regression line can describe the fuel consumption for any load of the generator. Eq. 29 represents the general form of this equation. Figure 19 shows an example of a graphic of fuel consumption by load of a generator with a regression line and equation.

$$R_{fuel} = a \times [L]^2 + [b \times L] + c \left[\frac{gal}{h}\right] \quad \textbf{Eq. 29}$$

where:

R_{fuel} - Fuel rate consumption [gal/h];

a, b & c - Constants.

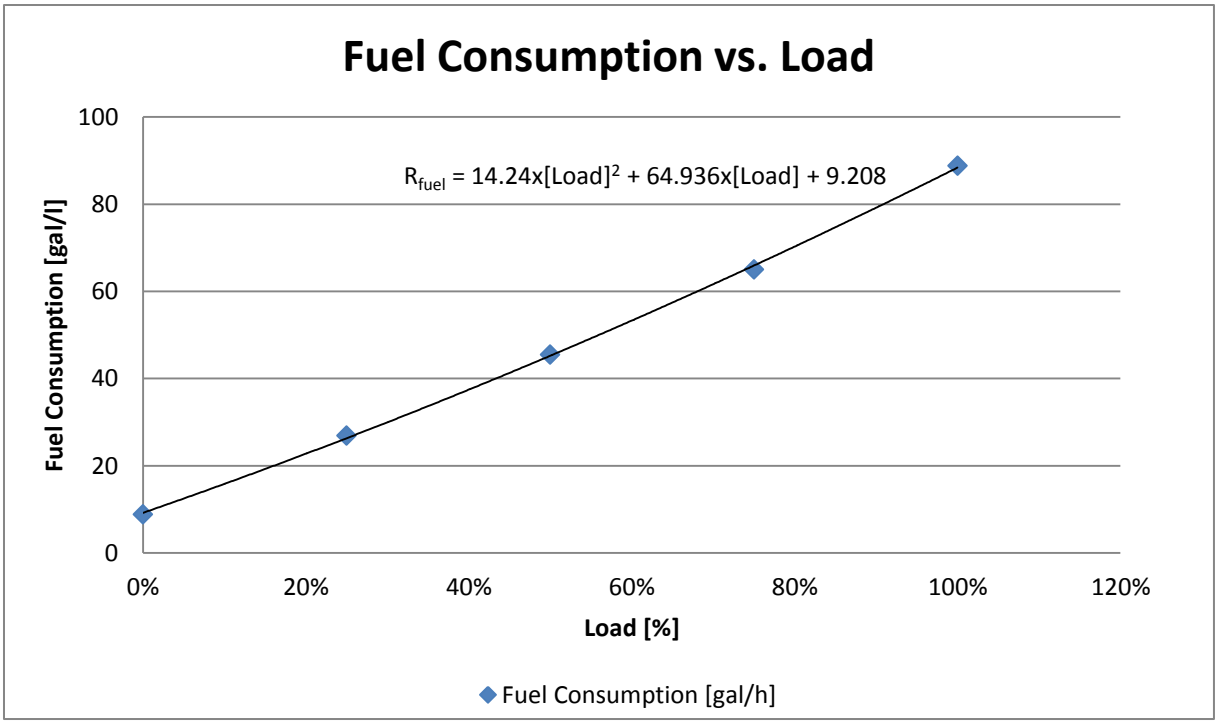

Figure 19: Fuel consumption variation by load.

The second step is to transform the total electrical power required by the rig (calculated by the Energy Consumption Mathematical Model, described in the previous section) into percentage of the total load of the generator. To accomplish that, the total electric power required by the rig is divided by the total power installed from the generators.

$$L = \frac{\boldsymbol{P}_{Total}}{\boldsymbol{P}_{\boldsymbol{inst.}}}[\%] \quad \textbf{Eq. 30}$$

where:

$P_{inst.}$ - Total power installed [W].

Applying the load percentage calculated by Eq. 30it is possible to obtain the fuel consumption per hour from the rig at that instantaneous moment. Using this concept in the developed model with drilling data it is possible to calculate the fuel consumption related to the time-span of the data frequency.

$$F_{Cons.} = R_{fuel} \times \mathrm{t}[gal] \quad \textbf{Eq. 31}$$

where:

$F_{Cons.}$ - Fuel Consumption [gal].

Table 10 presents the continuation of Table 3, which contains drilling data channels with a sampling frequency of 0.2 Hz. In Table 10the calculated total electrical power required by the rig is converted into load percentage of the generators. Then, the fuel consumed by the

generator to generate the required load is calculated based on 5s interval (referent to 0.2 Hz frequency) of the drilling data.

Table 10: Drilling data used in the model with 0.2 Hz sampling frequency.

Date	Time	Total Electrical Power [kW]	Load %	Fuel Rate [gal/h]	Fuel Consumption [gal]
14.09.2013	06:00:00	308.78	10.3%	21.00	0.06
14.09.2013	06:00:05	612.45	20.4%	21.00	0.06
14.09.2013	06:00:10	1327.11	44.2%	49.70	0.14
14.09.2013	06:00:15	1549.13	51.6%	56.99	0.16
14.09.2013	06:00:20	1509.38	50.3%	55.69	0.15
14.09.2013	06:00:25	1043.30	34.8%	40.38	0.11
14.09.2013	06:00:30	474.92	15.8%	21.00	0.06
14.09.2013	06:00:35	314.98	10.5%	21.00	0.06
14.09.2013	06:00:40	561.37	18.7%	21.00	0.06
14.09.2013	06:00:45	964.78	32.2%	37.80	0.10
14.09.2013	06:00:50	1061.73	35.4%	40.98	0.11
14.09.2013	06:00:55	1037.47	34.6%	40.18	0.11
14.09.2013	06:01:00	468.69	15.6%	21.00	0.06

The sum of the fuel consumptions for a period of 24 hours gives the amount of fuel consumed by the rig in one day. Thus, if real drilling data is used to feed the Energy Consumption Mathematical Model the results of the fuel consumption for the periods of 24 hours can be obtained. After, the result is compared with the real values of fuel consumed by the rig. This analysis is presented in the following section.

4.3.2 Model Predictions vs. Measured Data

To accomplish the validation of the model several wells are selected from the data base. Careful studies are performed to ensure that selected wells have all necessary input data for the models and the real values of fuel consumed by the rig for the further comparison (validation).

This section presents the comparison of results, for one well, of the calculated values of fuel consumed based on the real input data and the real values of fuel consumed daily by the drilling rig extracted from the drilling morning reports.

Appendix A– Fuel Consumption Results& Comparison0 contains the results of the other wells used in the validation of this model.

Table 11 presents the real values and the calculated values of the fuel consumed daily by the rig A from the Well A located in Texas in the Eagle Ford basin in the Blackhawk field (Well A).The blank cells in the table are because no information was found in the morning reports regarding these measurements.

Table 11: Real and calculated values of fuel consumed by the rig A.

Date	Calculated Fuel Consumption			Real Fuel Consumption		
	0-12h [gal]	12-24h [gal]	0-24h [gal]	0-12h [gal]	12-24h [gal]	0-24h [gal]
30.08.2013	1384	1561	2945	1049	1642	2691
31.08.2013	1809	1857	3666	1550	1935	3485
01.09.2013	992	492	1484	839	479	1318
02.09.2013	533	480	1014	382	385	767
03.09.2013	538	873	1410	193	971	1164
04.09.2013	1310	1277	2587	971	1360	2331
05.09.2013	1307	1411	2719	1148	1259	2407
06.09.2013	1518	1537	3055	1306	1714	3020
07.09.2013	1644	1548	3191	1359	1451	2810
08.09.2013	1620	1424	3044	1592	1359	2951
09.09.2013	1590	1443	3033	1213	1257	2470
10.09.2013	1406	572	1978	1230	581	1811
11.09.2013	511	509	1020	-	-	758
12.09.2013	525	552	1078	-	-	927
13.09.2013	611	501	1112	-	-	896

There are three basic approaches used in comparing a simulation model output behavior to the system output behavior: (1) to use of graphs to make a subjective decision, (2) to use of statistical tests to make an objective decision, and (3) to use of hypothesis tests to make an objective decision (Sargent, 2011).The approaches 1 and 2 are performed and presented in the following sub-sections.

4.3.2.1 Graphical Comparison of Data

For an easy visualization of the results few graphical comparisons are created. The figures below show these comparisons of the calculated vs. real values of fuel consumption for different periods (0-12h, 12-24h, and 0-24h).

Appendix A– Fuel Consumption Results& Comparison contains the graphical comparison of the result from other wells used in the model validation. Figure 20 presents the calculated and real values of fuel consumed in the period of 0 to 12 hours. The ordinate axis contains the daily fuel consumption values and the abscissa contains the time span of the well.

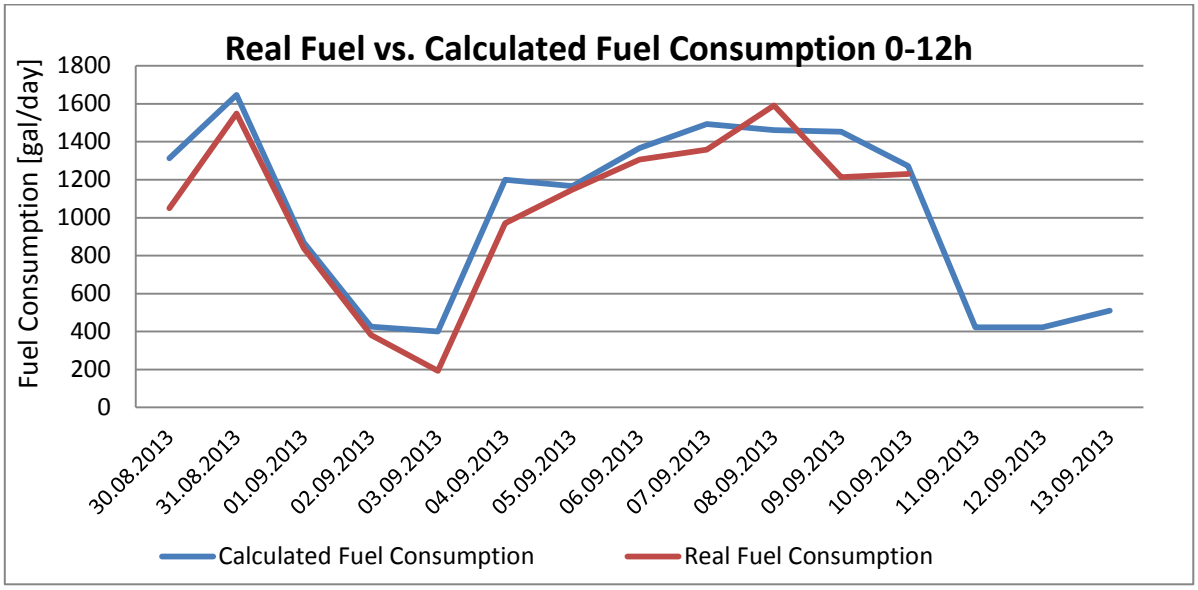

Figure 20: Real Fuel vs. Calculated Fuel Consumption referent to the period of 0-12h.

Figure 21 presents the same type of graphic as in Figure 20, with the difference that the calculated and real values of fuel consumed are referring to the period of 12 to 24 hours. The discontinuity of the red line for the last three days in both of first two figures is due to the blank cells in the Table 11, caused by the lack of information in the morning reports.

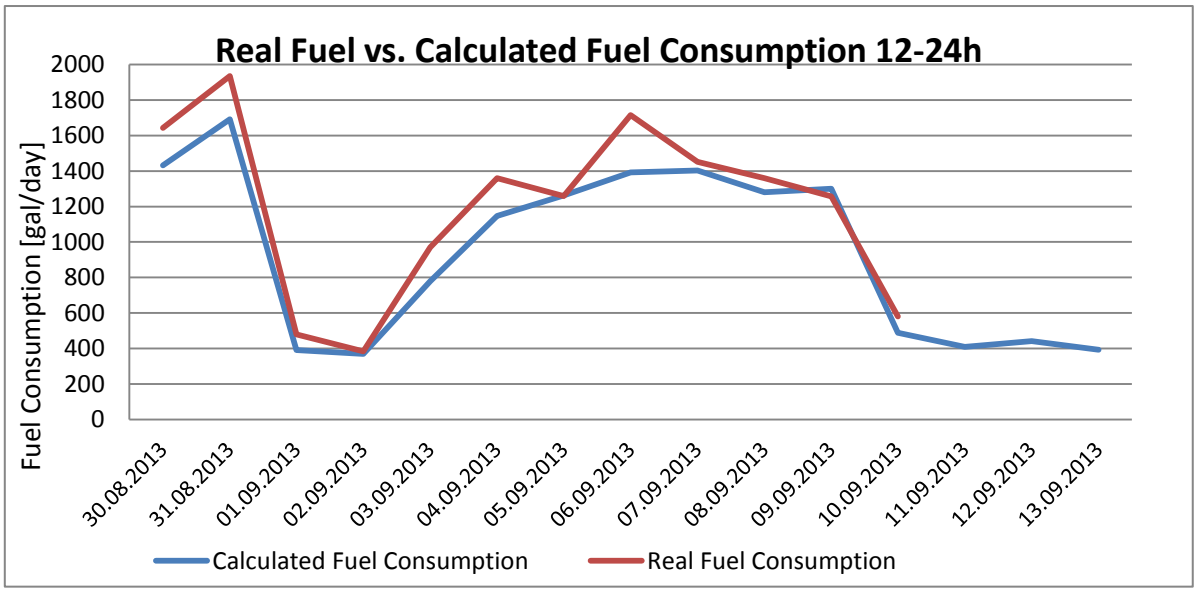

Figure 21: Real Fuel vs. Calculated Fuel Consumption referent to the period of 12-24h.

Figure 22 presents the same type of graphic as in the figures above, with the difference that the calculated and real values of fuel consumed are referring to the period of one full day.

By analyzing these graphics it is possible to observe a good correlation between the results. This correlation gives to the developed model a first credibility. The graphic comparison is not enough for validation of the model because it is a subjective analysis. Thus, more objective analysis needs to be performed with the use of statistical test in order to assure accuracy and credibility of the model.

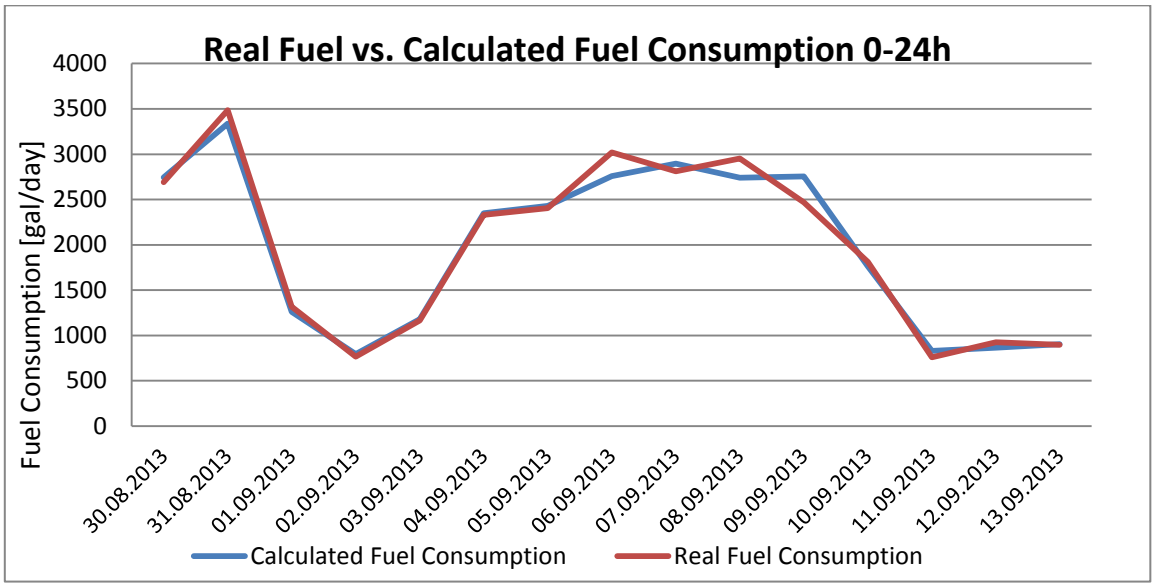

Figure 22:Real Fuel vs. Calculated Fuel Consumption referent to the period of 0-24h.

4.3.2.2 Coefficient of Determination - R^2

Literature studies are made in order to understand what types of statistical tests can be performed with the available data. The coefficient of determination (R^2) is chosen as suitable statistical tool to make an objective decision of the accuracy and credibility of the developed model.

In statistics, the coefficient of determination, denoted as R^2 and pronounced R squared, provides an estimate of the proportion of overlapping variance between two sets of numbers (i.e., the degree to which the two sets of numbers vary together), it indicates how well data points fit a line or curve (Brown, 2003). It is a statistic tool used in this thesis with the main purpose to provide a measure of how well the calculated fuel consumption values are correlated with the real fuel consumed values.

Coefficient of determination can take values as high as 1 when all the values are completely correlated, or as low as 0 when all the values are different (i.e. $0 \leq R^2 \leq 1$). In Figure 23 a scatter plot is presented, where the real fuel consumption values are plotted against the calculated fuel consumption values of the model for the Well A. A regression line is presented in the plot, and since the relation between the real fuel consumption values and the calculated fuel consumption values is linear, the regression line is forced through zero. The slope of the straight line shows the average ratio between the calculated values in relation to the real values. The closer the slope to 45°, the more precise the calculated

values comparing to the real ones. The result of coefficient of determination is also presented in the figure.

By simply moving the decimal point two places to the right, a coefficient of determination can be interpreted as the percentage of variance shared by two sets of values. So, a coefficient of determination of 0.975 can be interpreted as a proportion, or as 97.5%. It can be observed the great agreement between the calculated values in comparison to the real values.

As final part of the validation, Figure 24 presents the same plot as shown in Figure 23, with the difference that in this plot all the Wells (e.g. A, B, C) presented in Appendix A are shown together. The final result of the coefficient of determination can be extracted. Thus, it is possible to confirm the credibility and accuracy of the Energy Consumption Model with the use of the statistics tool, the coefficient of determination.

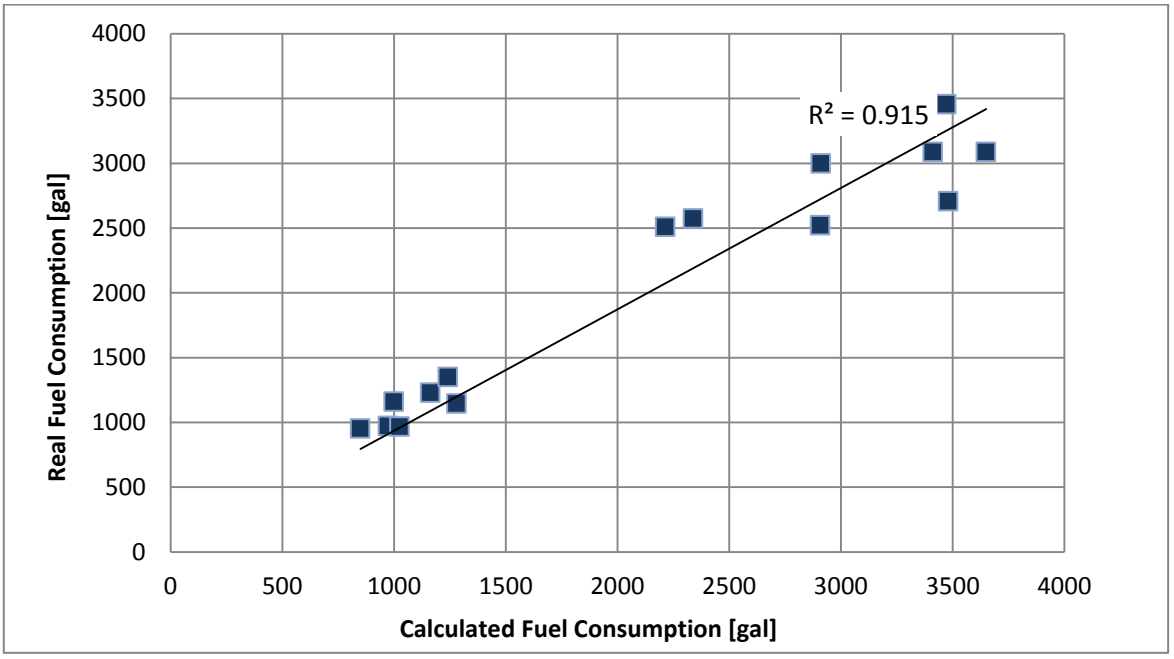

Figure 23: Coefficient of determination from real values vs. calculated values.

Some authors express concerns due to the reliability of this test. As Anscombe's quartet shows, a high R^2 can occur in the presence of misspecification of the functional form of a relationship or in the presence of outliers that distort the true relationship. To assure that this misspecification does not occur with the results of this thesis, a correlation check with the use of graphical comparison of the data (described in Section 4.3.2.1) is performed.

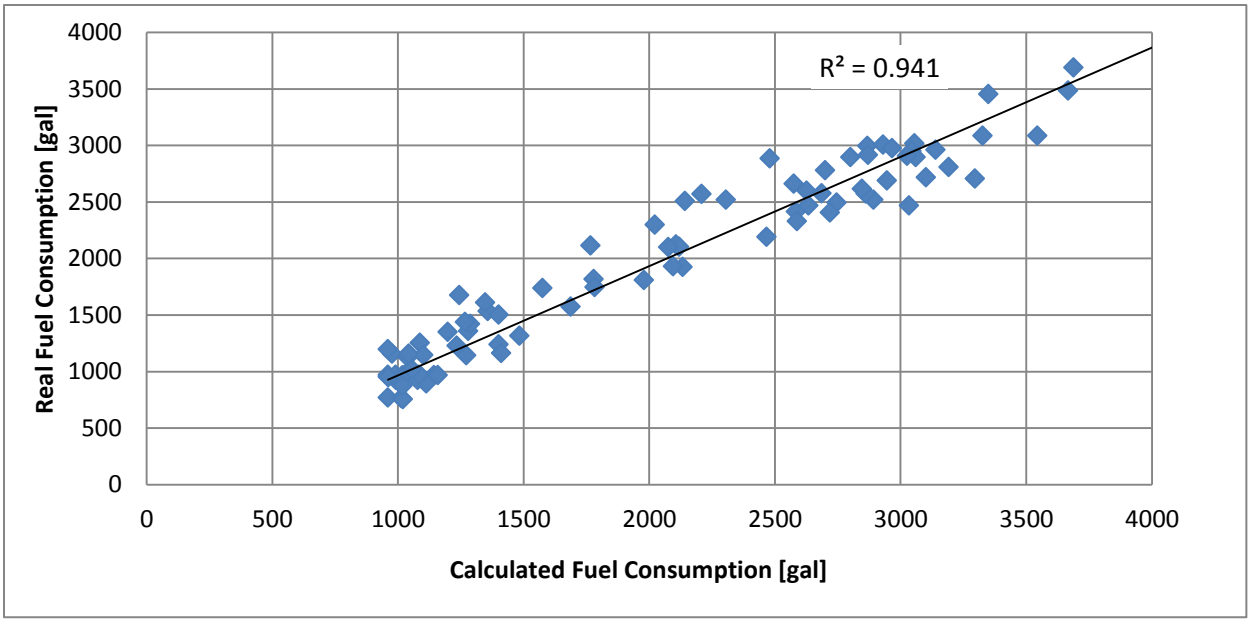

Figure 24: General coefficient of determination for the Energy Consumption Model.

4.4 Accreditation

The definition of accreditation provided by the USA Department of Defense is the following: “official certification that a model, simulation, or federation of models and simulations and its associated data are acceptable for use for a specific application”. Thus, the process of CV&V developed in this thesis assures the accreditation of the Energy Consumption Model.

As a final step to describe the exactly model development and CV&V process, Figure 25 is created. Figure 25 expands Figure 18, providing more detailed description of the whole process. Although Figure 18 is effective for explaining the major concepts involved in the CV&V model, several important activities are not shown. Figure 18 does not clearly represent 1) the various activities performed in the development of the model; 2) each process outcome achieved; and 3) an objective process for improving agreement between real data and the calculated data.

In Figure 25, the right branch illustrates the process of developing and exercising the model, and the left branch illustrates the process of obtaining relevant and high quality data to serve as input to the model and to accomplish the validation of the same. The closed boxes are the direct results of the process activities called process outcome. The connectors in black solid lines denote certain activities as to go from one outcome to the next. The connectors in dashed red lines mean the activities perform to evaluate the model and are called assessment activities.

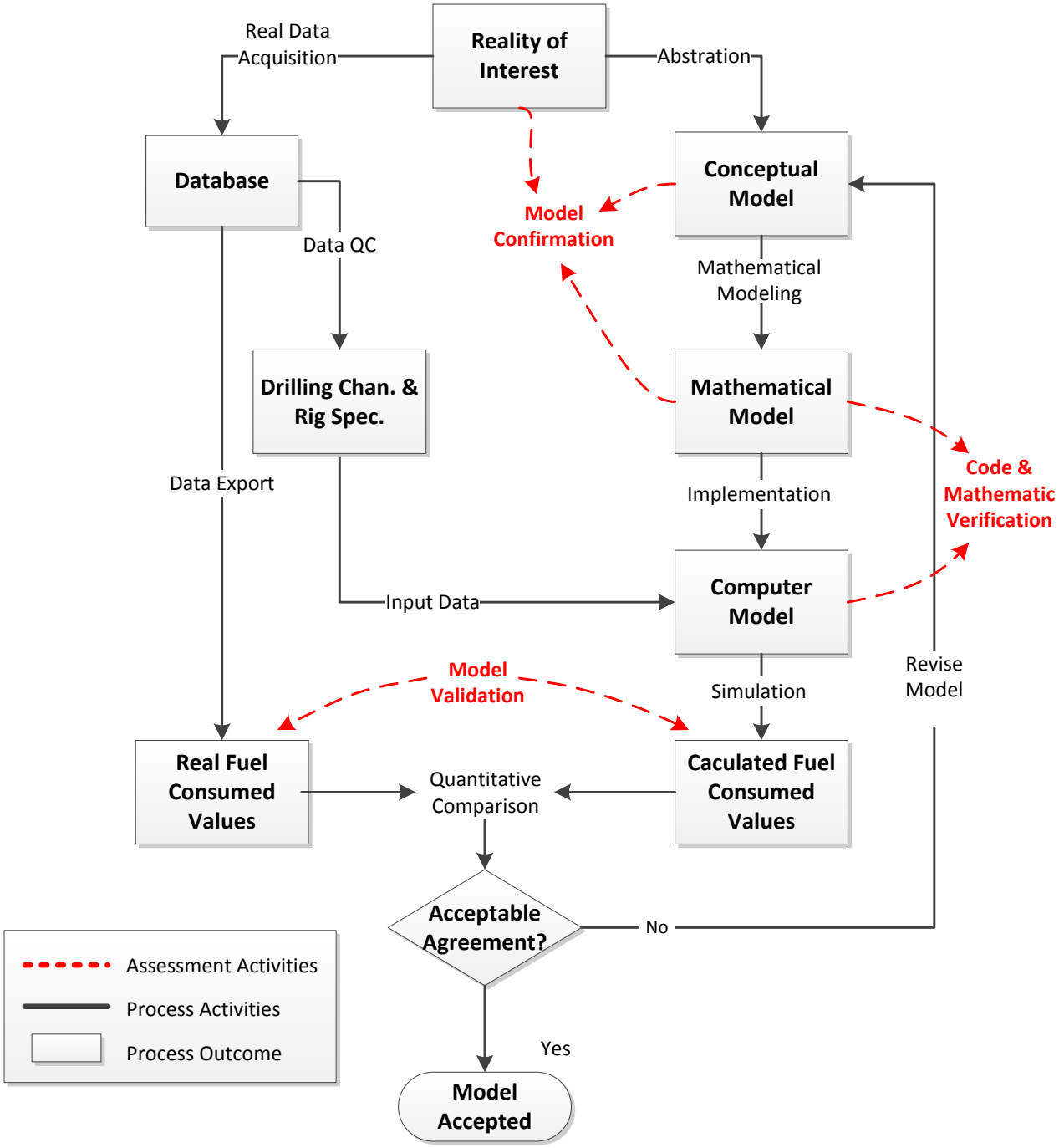

Figure 25: Detailed model development and CV&V. (Source: Modified from Thacker, 2004).

5. Conclusion

This chapter concludes the thesis with obtained results, difficulties/complications encountered during the thesis, and a short summary of the key recommendations for future applications. These recommendations were developed during the research based on the knowledge gathered.

1) The validation results of the developed energy consumption model confirm that the energy consumption of the top drive, mud pump and draw-works represent 88-95% of total daily drilling rig energy consumption. The mud circulation system takes the largest percentage of this energy use in the rig operation, thus improving the efficiency of the mud circulation system generates the highest impact on overall energy consumed. All the other equipment at the rig site (e.g. light, air conditioning system) consumes the remaining 12-5%.

2) Drilling data/parameters management: it was quite easy to obtain necessary data from the drilling channels (as they are common drilling parameters), although it was challenging to get correct specifications of the drilling rig equipment. Additionally, a drilling data quality check had to be performed in order to assure their sufficient quality.

3) As the inconsistent results of energy consumption were obtained due to incorrect information on the equipment power rating, the importance of the correct equipment power rating was noticed.

4) Significance of differentiating tripping-in and tripping-out operations was noticed for the energy consumption model of draw-works. During tripping-in operations the draw-works use only brakes when lowering the drill string, thus, only a fixed amount of power is required. During tripping-out operations the draw-works require power to lift the complete hookload of the system at a certain speed.

5) Moreover, it was noticed that the information on number of sheaves in the crown block/traveling block is not required for calculation of the mechanical power of the draw-works, as explained in Section3.3.3.2.

6) Based on the comparison of real vs. calculated figures of fuel consumption, the conceptual model was incrementally refined and improved. As a final figure the author obtained an R^2 of overall 94.1% of all the data used for the model validation.

As a final statement for the scope of this study, the thesis was a success since the objectives of the thesis were achieved. During the research, great understanding on the energy supply and energy consumption of a drilling rig was gained, as well as the specific knowledge on how to develop a model starting from the definition of the Reality of Interest until the Model Accreditation.

For future development and application of the research, the author recommends a more detailed analysis, which can be focused on:

1) to develop Energy (Energy efficiency) Based KPIs. The results of the energy consumption model combined with the rig states generated by the Automatic State Recognition system could define the energy consumed for each state. Further these states are combined in KPIs, thus providing the total energy consumed for each of the measured KPIs. Studies will be necessary to better understand the application of the results.
2) to create an operations breakdown according to energy demand of a future well based on a Drilling Data Simulator.
3) to use the total mechanical power output to quality check the drilling data: this value must never be greater than the equipment power rating specification.
4) to get more extensive set of Rig specifications to facilitate further study;
5) to use the Energy Based KPIs in order to quantify the amount of CO2, NO2 emission for each operation and create a comparison of the emissions for different sources of energy (e.g. electrical power grid, diesel motors, among others).

6. Bibliography

AIAA. (1998). *Guide for the Verification and Validation of Computational Fluid Dynamics Simulations.* Reston: AIAA-G-077-1998.

Al-Morakhi, R., Al-Shemali, A., Alsammak, I., Esterabadi, J., Martocchia, A., Ferroni, G., et al. (2013, 10 10). Real Time Advanced Flow Analysis for Early Kick/Loss Detection & Identification of Open Fractures. *SPE Kuwait Oil and Gas Show and Conference. SPE-167335-MS*, p. 6. Mishref, Kuwait: SPE.

Arnaout, A., Zoellner, P., Johnstone, N., & Thonhauser, G. (2013). Intelligent Data Quality Control of Real-time Rig Data. *SPE Middle East Intelligent Energy Conference and Exihibition* (p. 9). Dubai: SPE International.

Australian, D. o. (2008). *Mechanical & Electrical power relationships.* Brisbane: Australian Flexible Learning Framework.

Automation Consulting, LLC. (2011, 11 27). Variable Frequency Drives (VFDs). Nashville, Tennessee, USA. Retrieved from http://automationprimer.com/2011/11/27/variable-frequency-drives-vfds/

Azar, J. J., & Samuel, G. R. (2007). *Drilling Engineering.* Tulsa: PennWell Corporation.

Bentec Ltd. (2013). *Product information*. Retrieved 11 21, 2013, from Bentec Ltd.: http://www.bentec.com/equipment/mechanical-products/

Besore, S. (2010, 09 08). *MTU Detroit Diesel*. Retrieved 11 30, 2013, from Drilling Contractor: http://www.drillingcontractor.org/fuel-consumption-overload-capacity-among-critical-criteria-in-selection-of-generator-sets-6864

Bonitron Inc. (2014). Retrieved 11 21, 2014, from Bonitron Inc.: http://www.bonitron.com/industry-oil-drawworks.html

Brown, J. D. (2003, 03 1). The coefficient of determination. Manoa, Hawai, USA. Retrieved from http://jalt.org/test/bro_16.htm

Burt, C., Piao, X., Gaudi, F., Busch, B., & Taufik, N. (2006). *Electrical Motor Efficiency under Variable Frenquencies and Loads.* San Luiz Obispo: Irrigation Training & Research Center.

Cherutich, S. K. (2009). *Rig Selection and Comparison of Top Drive and Rotary Table Drive Systems for Cost Effective Drilling Preject in Kenya.* Naivasha: Kenya Electricity Generating Co, Ltd – KenGen.

China-OGPE. (2013). Retrieved 11 21, 2014, from China Manufacturers and Suppliers of Oil, Gas and Petrochemical Equipment: http://www.china-ogpe.com/

Dhayanandhan, G. (2011, 02 27). Calculating Consumption for a Diesel Generator. CHENNI, TAMIL NADU, INDIA. Retrieved from http://cr4.globalspec.com/thread/76597

Diesel Service & Supply. (2013). Approximate Diesel Fuel Consumption Chart. Retrieved from http://www.dieselserviceandsupply.com/Diesel_Fuel_Consumption.aspx

DrillingFormula. (2010, 04 10). *Drilling Formulas*. Retrieved 11 25, 2013, from Frictional Pressure Loss Components in the Rig Circulating System: http://www.drillingformulas.com/frictional-pressure-loss-components-in-the-rig-circulating-system/

Florence, F., & Iversen, F. (2010). Real-time models for drilling process automation: Equations and applications. *IADC/SPE Drilling Conference and Exhibition.*

GlobalSpec Inc. (2013). Retrieved 01 12, 2015, from IHS GlobalSpec: http://www.globalspec.com/

Heinemann, Z. E. (2005). *Fluid Flow in Porous Media.* Leoben: Montanuniversität.

Lyons, W. C. (1996). *Standard Handbook od Petroleum & Natural Gas Engineering.* Houston: Gulf Publishing Company.

Mathis, W., & Thonhauser, G. (2007). Mastering Real-Time Data Quality Control - How To Measure and Manage the Quality of (Rig) Sensor Data. *Middle East Drilling Technology Conference & Exihibition* (p. 10). Cairo: SPE/IADC.

McCoy, G. A., Litman, T., & Douglass, J. G. (1993). *Energy-Efficient Electric Motor Selection Handbook.* Olympia,: Washington State Energy Office.

NOV. (2014). Retrieved 01 12, 2015, from National Oilwell Varco: http://www.nationaloilwell.com/

Oil & Gas Journal. (2006, 02 20). Retrieved 11 24, 2014, from Oil & Gas Journal: http://www.ogj.com/articles/print/volume-104/issue-7/special-report/nabors-drilling-designs-new-ac-rigs.html

Paez, T. L. (2009). Introduction to Model Validation. *IMAC-XXVII.* Orlando: Society for Experimental Mechanics Inc.

Prassl, W. F. (2002). *Drilling Engineering.* Curtin: Curtin University of Technology.

Rajput, R. (1998). *A Textbook of Hydraulic Machines in SI Units.* New Delhi: S. Chand & Company Pvt.

Rigmaster Machinery Ltd. (2013). Retrieved 01 12, 2015, from RigMaster: http://www.rigmastermachinery.com/index.php?id=65

Saidur, R. (2009, 10 20). A review on electrical motors energy use and energy savings. *Renewable and Sustainable Energy Reviews*, pp. 877-898.

Sargent, R. G. (2011). Verification and Validation of Simulation Models. *Winter Simulation Conference.* Phoenix: Institute of Electrical and Electronics Engineers.

Schlumberger. (2012). *The Expanding Role of Mud Logging.* Oilfield Review.

Singh, S. K. (2003). *Industrial Instrumentation & Control - 2 ed.* New Delhi: Tata McGraw-Hill Publishing Company Limited.

Sivasankaran, G. A., & Jain, S. (1988, July). Performance of Diesel Engines at High Altitudes. *Def Sci J, Vol 38, No. 3*, pp. pp. 301-313.

Sola, A. V., & Mota, C. M. (2011, 12 17). A multi-attribute decision model for portfolio selection aiming to replace technologies in industrial motor systems. *Energy Conversion and Management*, pp. 97-106.

Thacker et al., B. H. (2004). *Concepts of Model Verification and Validation.* Los Alamos: Los Alamos National Laboratory.

Waide, P., & Brunner, C. U. (2011). *Energy-Efficiency Policy Opportunities for Electric Motor-Driven Systems.* Paris: International Energy Agency.

Appendix A– Fuel Consumption Results& Comparison

This appendix contains the results of the calculated values of fuel consumed based on the real input data and the real values of fuel consumed daily by the drilling rig extracted from the drilling morning reports for all the other wells used to validate this model.

Well B

Date	Calculated Fuel Consumption			Real Fuel Consumption		
	0-12h [gal]	12-24h [gal]	0-24h [gal]	0-12h [gal]	12-24h [gal]	0-24h [gal]
30.08.2013	450	486	937	-	767	1149
31.08.2013	976	976	1952	-	796	2101
01.09.2013	964	940	1904	-	-	-
02.09.2013	546	510	1055	-	471	1439
03.09.2013	1236	1273	2509	-	1360	2898
04.09.2013	1249	1308	2557	-	2617	2617
05.09.2013	1444	1175	2619	-	-	-
06.09.2013	1283	1444	2727	-	-	2909
07.09.2013	1391	1448	2839	-	-	2962
08.09.2013	1313	493	1807	-	-	2299
09.09.2013	370	446	816	-	-	972
10.09.2013	1284	1530	2815	-	-	2719
11.09.2013	1529	1155	2684	-	-	2978
12.09.2013	435	423	858	-	-	1020
13.09.2013	428	447	875	-	-	1159
14.09.2013	411	365	776	-	-	956

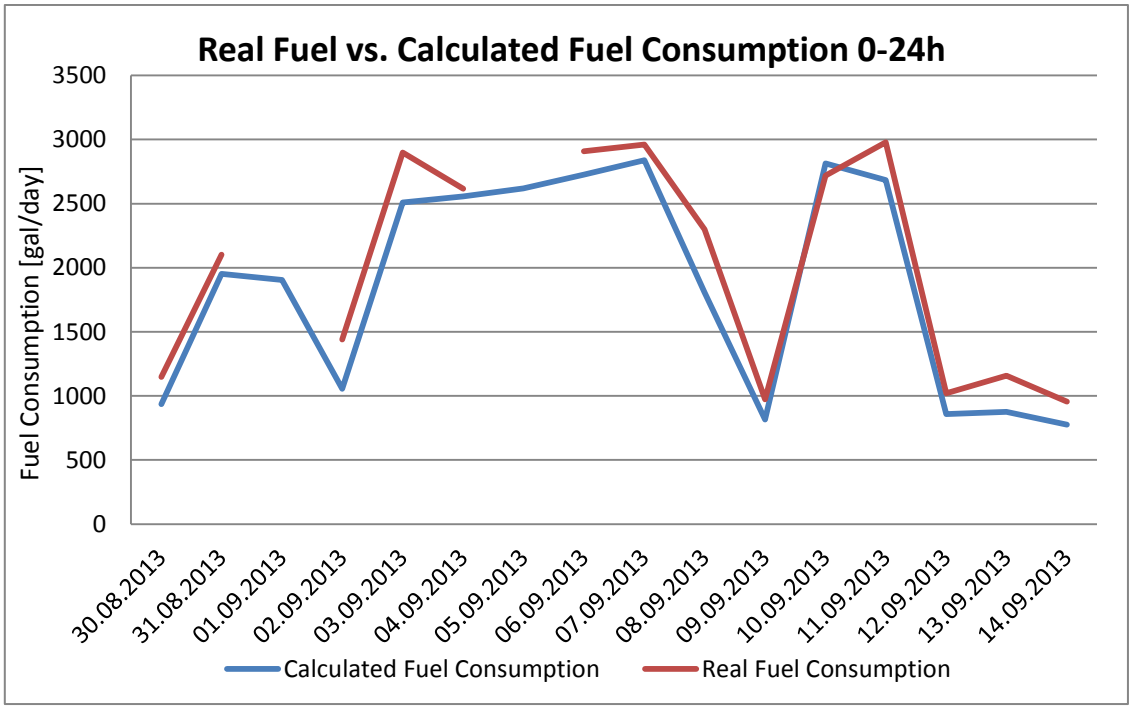

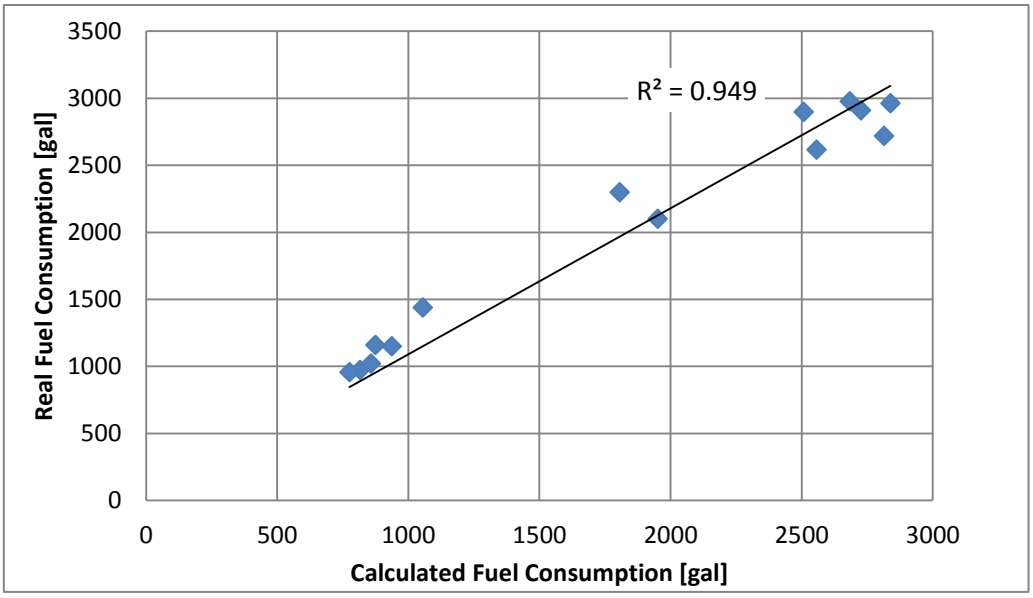

Well C

Date	Calculated Fuel Consumption			Real Fuel Consumption		
	0-12h [gal]	12-24h [gal]	0-24h [gal]	0-12h [gal]	12-24h [gal]	0-24h [gal]
10.09.2013	377	1128	1505	572	1002	1574
11.09.2013	1629	1874	3503	1698	1991	3689
12.09.2013	1322	1426	2748	1303	1706	3009
13.09.2013	1846	971	2817	1779	1118	2897
14.09.2013	397	418	816	472	491	963
15.09.2013	377	403	780	409	468	877
16.09.2013	671	1220	1891	732	1199	1931

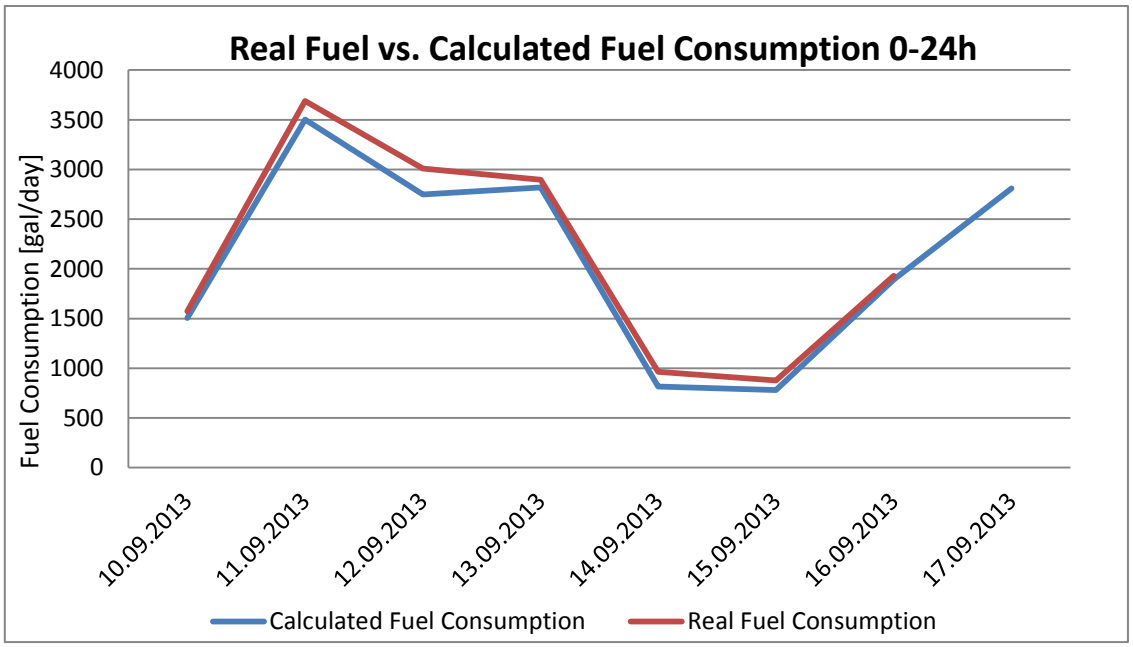

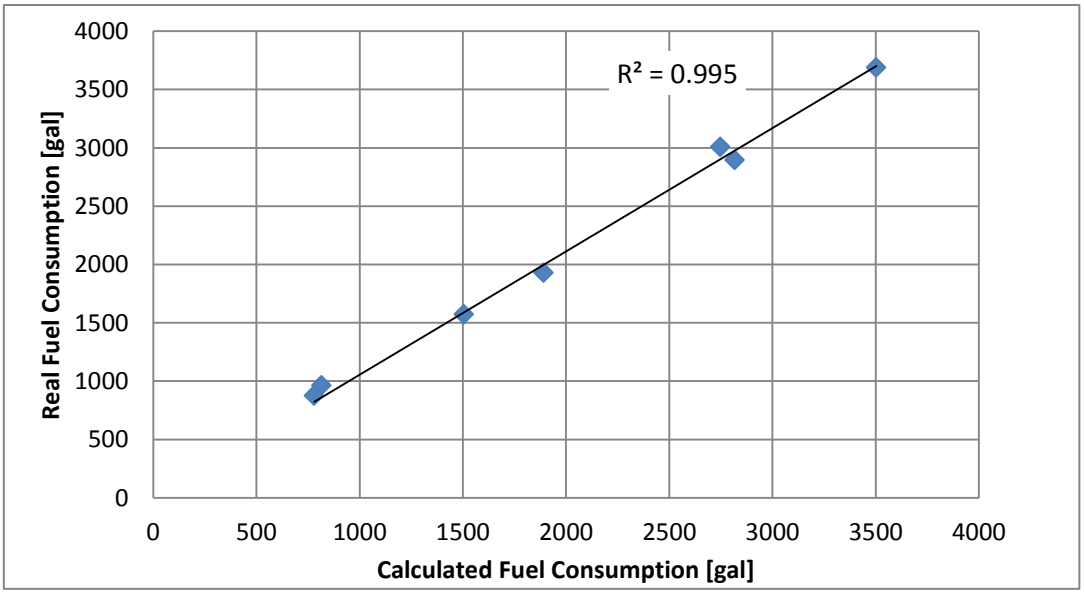

Well D

Date	Calculated Fuel Consumption			Real Fuel Consumption		
	0-12h [gal]	12-24h [gal]	0-24h [gal]	0-12h [gal]	12-24h [gal]	0-24h [gal]
07.08.2013	1178	1318	2496	1344	1230	2574
08.08.2013	1294	639	1933	2072	193	2265
09.08.2013	1021	1220	2242	1060	1115	2175
10.08.2013	1184	1277	2461	1479	949	2428
11.08.2013	1386	1421	2807	1549	1164	2713
12.08.2013	1466	914	2380	1723	776	2499
13.08.2013	606	520	1126	778	387	1165

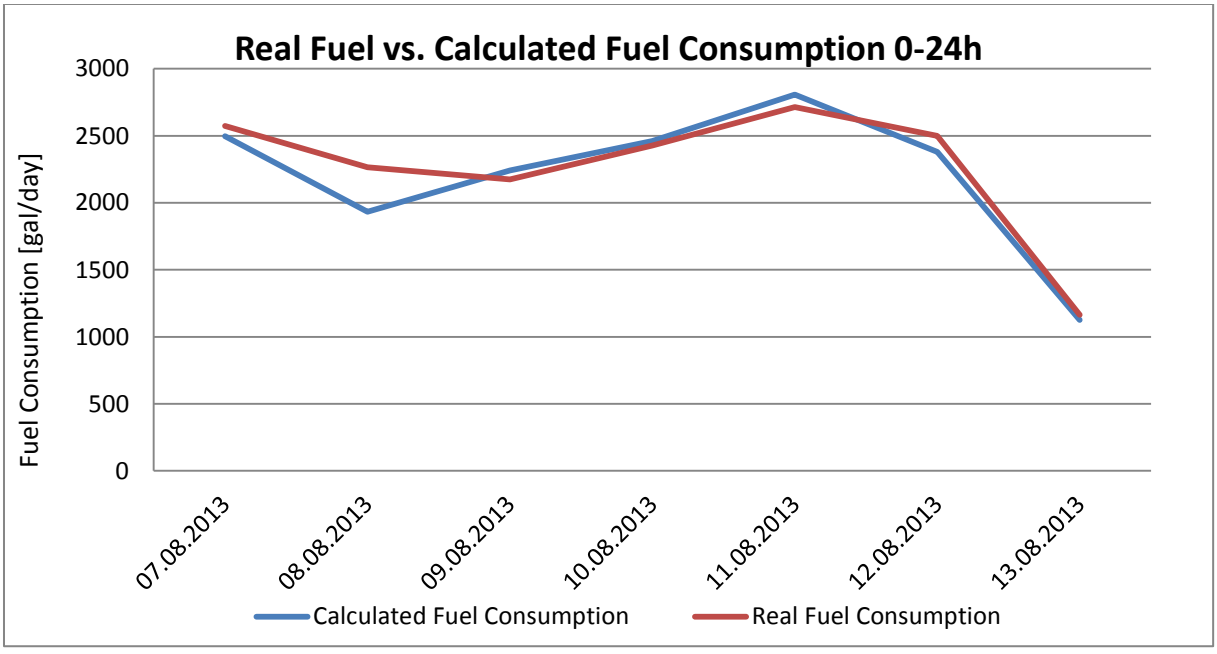

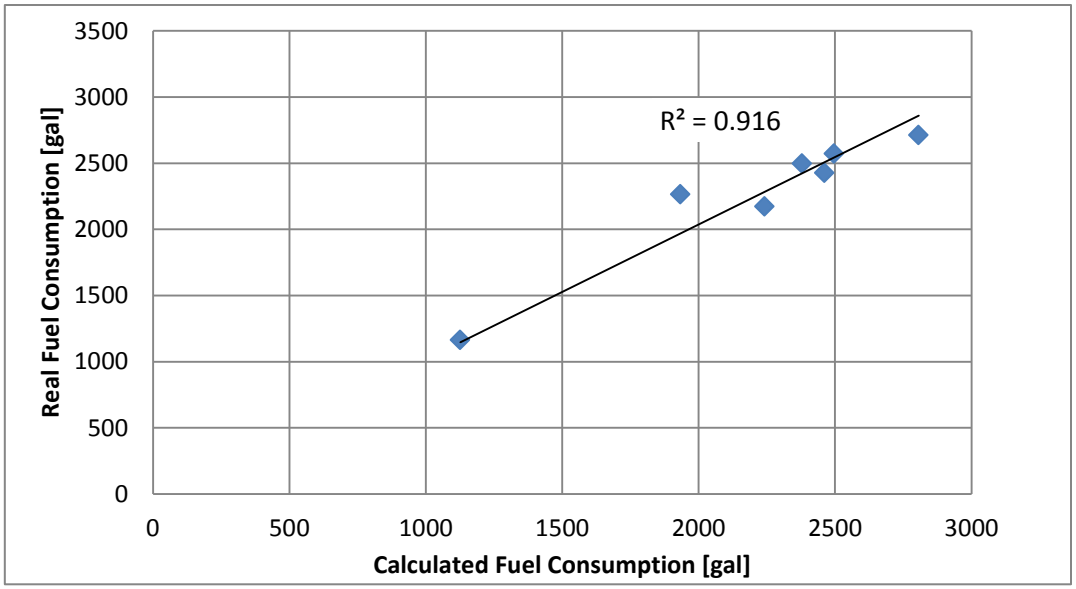

Well E

Date	Calculated Fuel Consumption			Real Fuel Consumption		
	0-12h [gal]	12-24h [gal]	0-24h [gal]	0-12h [gal]	12-24h [gal]	0-24h [gal]
20.07.2013	754	621	1375	-	-	1612
21.07.2013	447	446	893	-	-	-
22.07.2013	412	412	824	-	-	-
23.07.2013	419	421	839	-	-	-
24.07.2013	621	1208	1829	582	1166	1748
25.07.2013	966	1210	2175	765	1160	1925
26.07.2013	1371	1116	2487	1553	1333	2886
27.07.2013	471	1058	1529	574	1166	1740
28.07.2013	1240	1348	2588	933	1537	2470
29.07.2013	1388	1478	2865	1070	1505	2575
30.07.2013	1358	802	2161	1334	772	2106
31.07.2013	531	845	1376	521	721	1242
01.08.2013	1318	1376	2693	1273	1305	2578
02.08.2013	630	481	1110	527	727	1254
03.08.2013	510	519	1029	560	569	1129

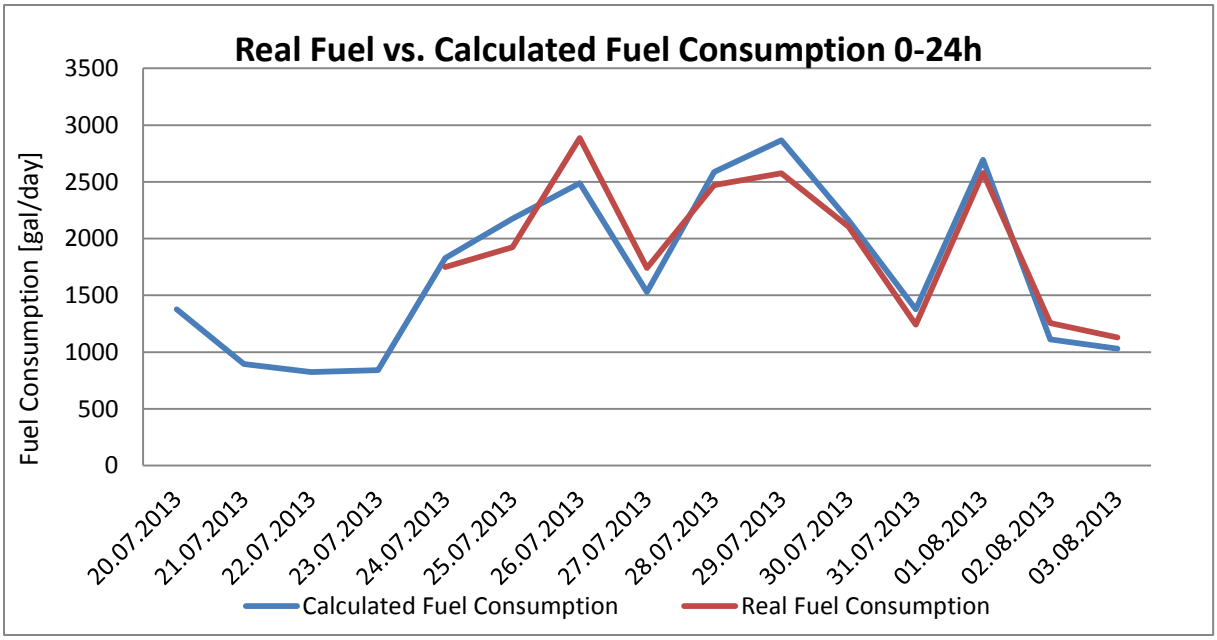

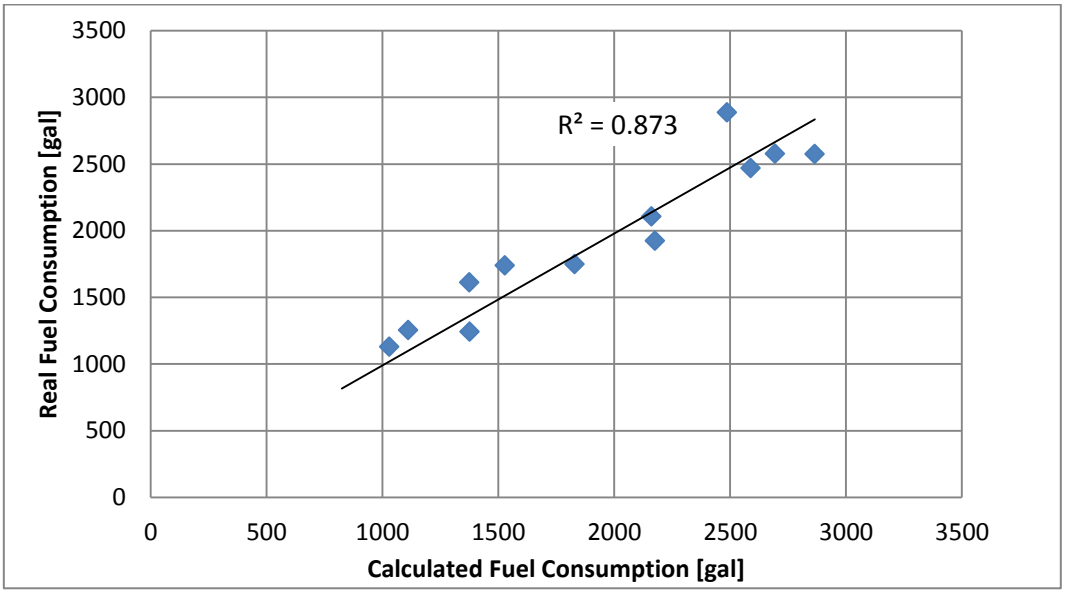

Well F

Date	Calculated Fuel Consumption			Real Fuel Consumption		
	0-12h [gal]	12-24h [gal]	0-24h [gal]	0-12h [gal]	12-24h [gal]	0-24h [gal]
17.08.2013	449	830	1280	-	-	1146
18.08.2013	1066	1273	2338	-	-	2573
19.08.2013	1327	888	2215	-	-	2510
20.08.2013	493	507	999	-	-	1160
21.08.2013	428	422	849	-	-	953
22.08.2013	481	682	1163	-	-	1230
23.08.2013	1442	1469	2910	-	-	2997

24.08.2013	1614	2037	3651	-	-	3088
25.08.2013	1813	6040	7853*	-	-	-
26.08.2013	2262	1218	3481	-	-	2707
27.08.2013	1381	1527	2908	-	-	2522
28.08.2013	1702	1709	3411	-	-	3088
29.08.2013	1700	1773	3473	-	-	3455
30.08.2013	750	492	1242	-	-	1351
31.08.2013	439	534	973	-	-	973
01.09.2013	555	470	1025	-	-	966

* This value clearly shows an error in the drilling data used to calculate the fuel consumption.

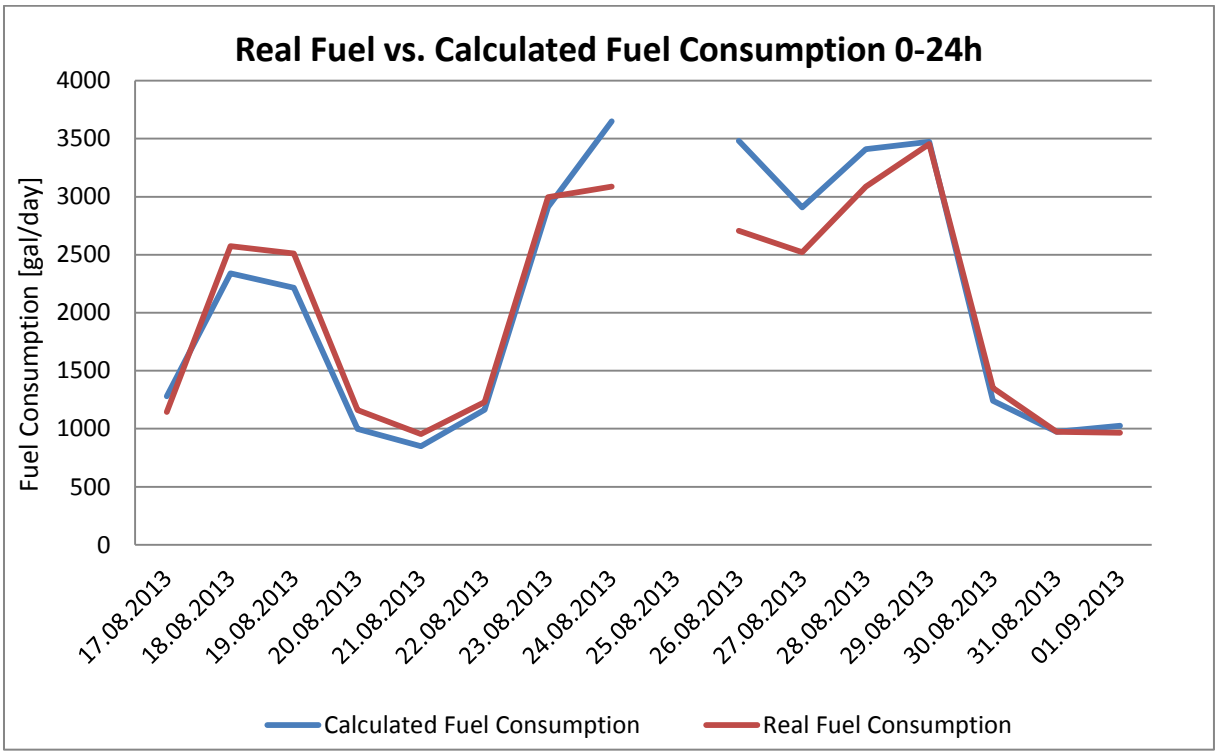

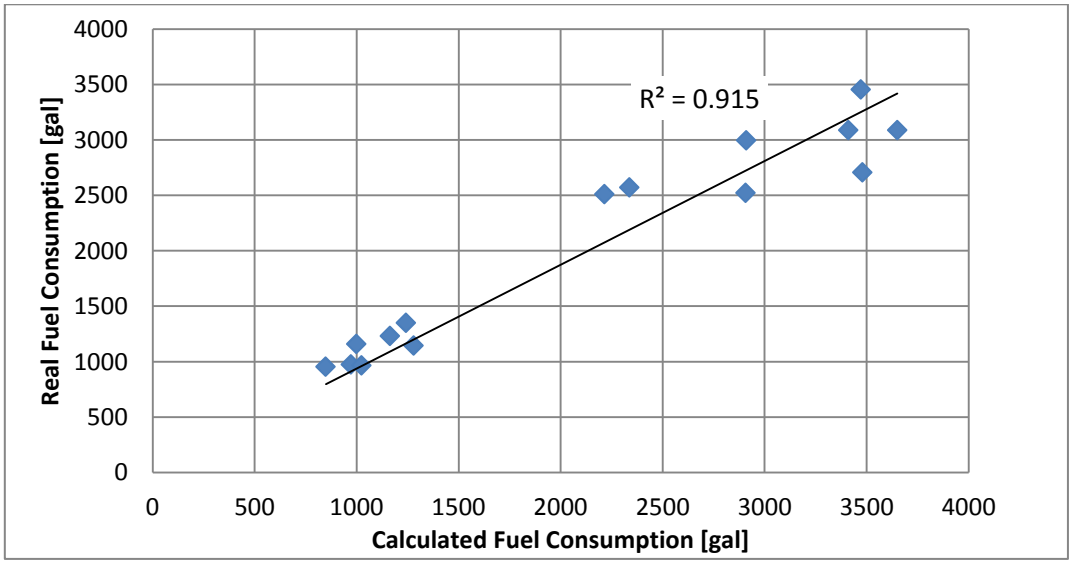

Well G

Date	Calculated Fuel Consumption			Real Fuel Consumption		
	0-12h [gal]	12-24h [gal]	0-24h [gal]	0-12h [gal]	12-24h [gal]	0-24h [gal]
19.06.2013	787	378	1165	-	-	1537
20.06.2013	365	363	728	-	-	973
21.06.2013	364	364	727	-	-	772
22.06.2013	367	521	888	-	-	957
23.06.2013	990	1069	2059	-	-	2125
24.06.2013	1251	1231	2481	-	-	2599
25.06.2013	1218	421	1639	-	-	2115
26.06.2013	402	433	836	-	-	-
27.06.2013	367	364	731	-	-	-
28.06.2013	364	394	758	-	-	927
29.06.2013	513	3299	-	-	-	-
30.06.2013	1466	4108	-	-	-	-
01.07.2013	1225	2960	-	-	-	-
02.07.2013	2137	505	2642	-	-	-
03.07.2013	378	554	932	-	-	970
04.07.2013	555	519	1074	-	-	1359
05.07.2013	691	404	1096	-	-	1423
06.07.2013	364	373	737	-	-	-
07.07.2013	602	654	1256	-	-	1505
08.07.2013	400	429	829	-	-	950
09.07.2013	408	445	853	-	-	973
10.07.2013	394	563	957	-	-	969
11.07.2013	565	1056	1621	-	-	1818
12.07.2013	564	474	1038	-	-	1677
13.07.2013	1137	1145	2282	-	-	2192
14.07.2013	783	406	1189	-	-	-
15.07.2013	401	895	1296	-	-	-
16.07.2013	1203	1184	2387	-	-	-
17.07.2013	1193	1206	2399	-	-	2663
18.07.2013	1152	1246	2397	-	-	2417
19.07.2013	716	433	1149	-	-	-
20.07.2013	1047	1277	2324	-	-	-
21.07.2013	1272	1298	2569	-	-	2494
22.07.2013	817	1327	2145	-	-	2520
23.07.2013	1343	1193	2536	-	-	2782

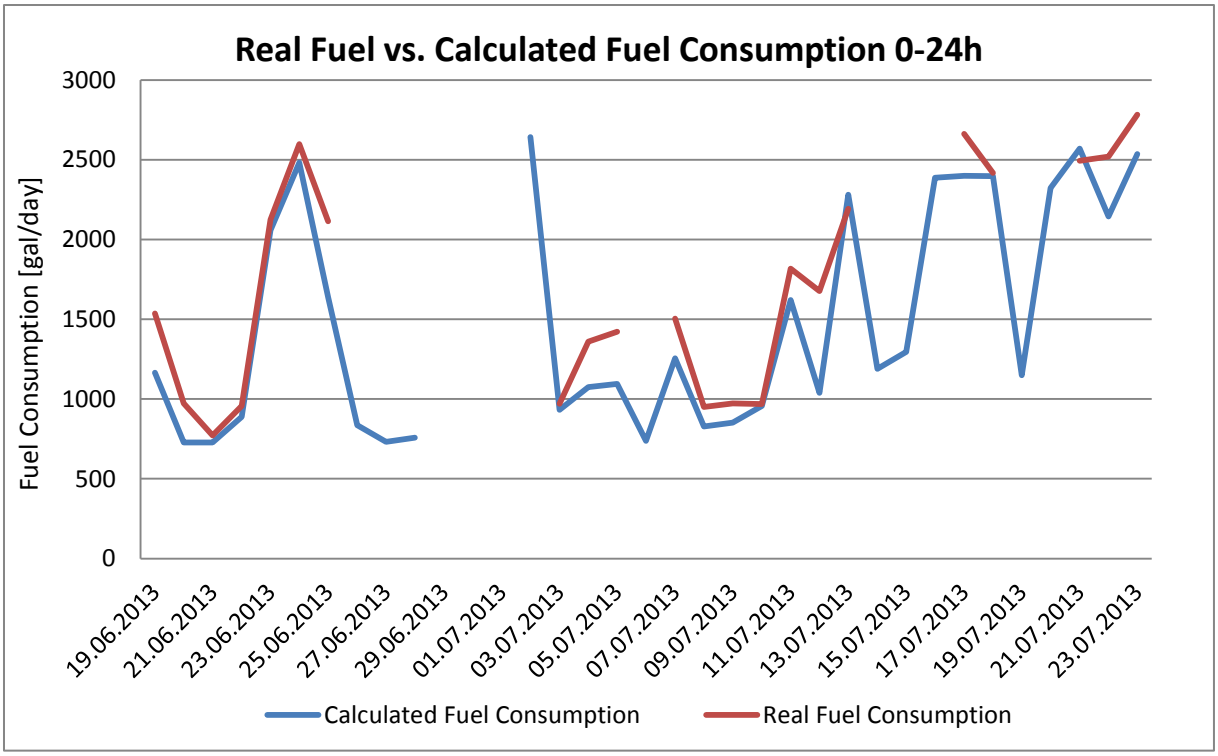
Real Fuel vs. Calculated Fuel Consumption 0-24h
Fuel Consumption [gal/day]
3000
2500
2000
1500
1000
500
0
19.06.2013
21.06.2013
23.06.2013
25.06.2013
27.06.2013
29.06.2013
01.07.2013
03.07.2013
05.07.2013
07.07.2013
09.07.2013
11.07.2013
13.07.2013
15.07.2013
17.07.2013
19.07.2013
21.07.2013
23.07.2013
Calculated Fuel Consumption
Real Fuel Consumption

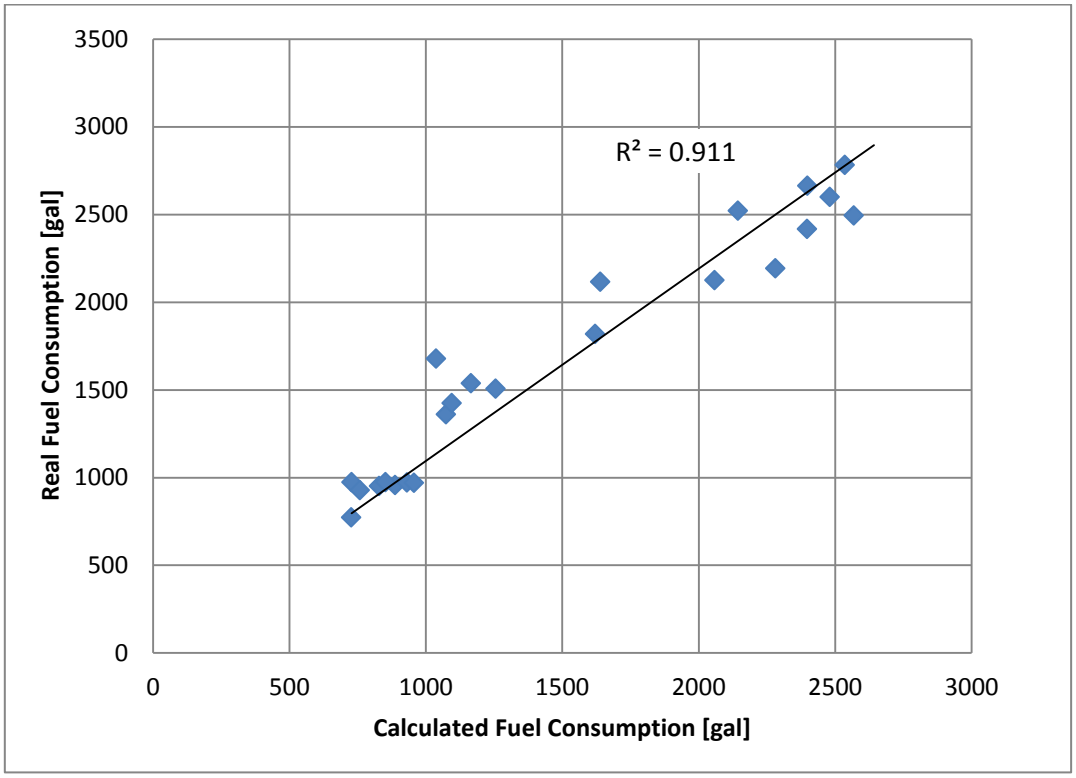
R² = 0.911
Real Fuel Consumption [gal]
Calculated Fuel Consumption [gal]
3500
3000
2500
2000
1500
1000
500
0
0
500
1000
1500
2000
2500
3000

LIST OF SYMBOLS

E - Energy [J];

P_{ele} - Electrical Power [W];

t - Time [s];

$P_{mec\ or\ hyd}$ - Mechanical or Hydraulic Power [W];

$\eta_{overall}$ - Overall efficiency [%];

η_{motor} - Motor efficiency [%];

η_{VFD} - VFD efficiency [%];

$\sum Losses$ - Losses [W];

$\sum Losses_{Overall}$ - Overall Losses [W];

$\sum Losses_{Motor}$ - Motor Losses [W];

$\sum Losses_{VFD}$ - VFD Losses [W];

f - Force [N];

d - Distance [m];

T - Torque [N.m];

n - Rotation [rpm];

P - Pressure [Pa];

Q - Flow In [m3/h];

g - Gravity [m/s2];

ρ - Fluid density [kg/m3];

η - Efficiency [%];

P_{output} - Output power [W];

P_{input} - Output power [W];

$P_{equip.}$ - Equipment power [W];

L - Load [%];

$P_{Top\ Drive}$ - Top drive power [W];

$P_{Mud\ Pumps}$ - Mud Pumps power [W];

η_m - Mechanical efficiency;

η_h - Hydraulic efficiency;

η_v - Volumetric efficiency;

η_f - Friction efficiency;

w - Specific work from the pump or fan [W];

w_L - Specific work lost due to hydraulic effects [W];

P - Power transferred from the motor to the shaft [W];

P_L - Power lost in the transmission [W];

q - Volume flow out of the pump or fan [W];

q_L - Leakage volume flow [W];

V_{linear} - Fast line linear velocity [m/s];

BH - Block height [m];

Δt - Time difference [s];

$N_{sheaves}$ - Number of sheaves;

ω - Angular velocity [rpm];

r - Drum radius [m];

hk - Hookload [kg];

$P_{Draw-works}$ - Draw-works power [W];

$P_{Extra\ Equip.}$ - Extra equipment power [W];

$P_{inst.}$ - Total power installed [W];

$p_{Extra\ Equip.}$ - Extra equipment load [%];

P_{Total} - Total electrical power [W];

R_{fuel} - Fuel rate consumption [gal/h];

$a, b\ \&\ c$ - Constants;

$P_{inst.}$ - Total power installed [W];

$F_{Cons.}$ - Fuel Consumption [gal].